5-3 Sampling Results

Sampling using arm dredge (AD) and large gravity corer (LC) was carried out on every seamounts for the purpose of collecting manganese crusts. Sampling sites were designed to cover the whole seamount from the summit to the lower flank. These localities were selected for the target where the MBES sound image showed high acoustic pressure (manganese crusts are exposed on the seafloor). Some of the sampling sites were selected from the seafloor observation by FDC. The total number of sampling sites was 119 points; 78 points by AD and 41 by LC.

The followings are the description of the collected manganese crusts. The sampling locations are shown in Figures 4-2-1 (1) to (9), the collected materials are listed in Tables 4-2-1 (1), (2), and the summary of the sampling of manganese crusts is laid out in Table 5-3-1.

(1) Arm dredge (AD)

AD sampling was carried out at 78 points of all nine seamounts. At two localities, the amount of manganese crusts collected was not sufficient for shipboard chemical analysis. Sampling localities were designed to wholly cover the seamount from the flat summit to the lower flank.

Photographs of typical manganese crusts collected by AD are shown in Figures 5-3-1 (1), (2), and the results of the sampling are laid out in Appendix Tables 2 (1) to (3).

1) Characteristics of manganese crusts by classification

a) Crust (Fig. 5-3-1 (1), Photo Nos. 5 to 8)

The surfaces form botryoidal (Fig. 5-3-1 (1), Photo 1), granule (Fig. ib., Photo 3), stromatolite (Fig. ib., Photo 2), or porous irregular structure. The thickness of manganese crusts ranges from thin coating under 1 mm to a maximum of 105 mm. The crust is divided into one to three layers, and the thicker one tends to contain the more layers. The substrates are mainly basaltic pyroclastic rocks and basalt breccia, with smaller amount of volcanic conglomerate, limestone, basalt and others.

b) Cobble crust (Fig. 5-3-1 (2), Photo Nos. 9 to 12)

The surface form botryoidal, granule, smooth (Fig. 5-3-1 (1), Photo 4), or porous irregular structure. The thickness of manganese crusts ranges from thin coating under 1mm to a maximum of 100 mm. The crust is divided into one to three layers, and the thicker one tends to contain the more layers. The substrates are basalt, basaltic pyroclastic rocks, sandstone, limestone, and others.

c) Nodule (Fig. 5−3−1 (2), Photo Nos. 13 to 16)

The surface features are botryoidal, granule to smooth. The thickness of manganese crusts ranges from thin coating under 1 mm to a maximum of 30 mm. Most of the crusts are divided into one to two layers, but in rare cases into three layers. The substrate nuclei consist of various rocks; basalt, basaltic pyroclastic rocks, sandstone, limestone, phosphorite manganese crust fragments, foraminifera sand, and others. Also the nodules often lack nuclei.

2) Occurrence by seamounts

The manganese crusts collected from each seamount are briefly described below.

a) MS01

The average thickness of manganese crusts is 30 mm with a maximum of 90 mm. This average is the thickest among all seamounts surveyed. All sampling localities have average thickness over 10 mm, and relatively thick manganese crusts were collected throughout this seamount. The thickest manganese crust was collected at the northeast margin of the flat summit (96SMS01AD11). Thin coating of manganese crusts is observed throughout the flanks. There is no clear correlation between the crust thickness and the water depth or the locality of sampling site. Small amount of nodules was collected at the flat summit and the gentle lower flank.

A crust with stromatolitic surface structure, whose column was 3 cm high and 2 cm diameter, was collected in 96SMS01AD10. A big cobble crust, whose crust thickness was thin coating to 50 mm and whose long axis was 90 cm and whose substrate was basalt breccia, was collected in 96SMS01AD12. Such large cobble crusts are observed by FDC observation and are not uncommon. Weakly consolidated brown mud blocks, covered by thin coating of manganese crusts around 1 mm thick, was collected at the deepest sampling site 96SMS01AD09 (3,229 m water depth) in this seamount.

b) MS02

The average thickness of manganese crusts is 25 mm with a maximum of 105 mm. This maximum value is the largest among all seamounts surveyed. The thickest manganese crust was collected at the upper flank on the northern part of the seamount (96SMS02AD07). There is no clear correlation between the crust thickness and the water depth or the locality of sampling site. Small amount of nodules was collected mainly on the flat summit.

Cobble crusts, whose nuclei were formed by the combination of several nodules and a basalt gravel, were collected in 96SMS02AD13. Such phenomenon, that nodules, cobble crusts and rock fragments are combined to form a new nucleus and larger cobble crust is made up, is not uncommon. A nodule with a maximum thickness 30 mm and a cobble crust with a thickness 65 mm were collected in 96SMS02AD18. Both nodule and cobble crust have the same sectional features

Table 5-3-1 Summary results of manganese crusts sampling

Seamount	Sampling Station				Manganese Crust Thickness (mm)		Mean (wt %) and Standard Deviation of Five Major Elements on Chemical Analysis									
	No. of Station	Water Depth (m)					No. of Sample	Co		Ni		Cu		Mn		Fe	
		Max.	Min.	Mean	Max.	Average		Mean	S. D.	Mean	S. D.	Mean	S. D.	Mean	S. D.	Mean	S. D.
MS01	11	3,227	1,225	1,787	90	30	40	0.67	0.17	0.62	0.20	0.12	0.06	22.59	2.66	13.96	3.48
MS02	16	3,091	1,525	1,927	105	25	46	0.70	0.28	0.54	0.12	0.10	0.04	22.08	3.73	13.61	3.03
MS03	7	2,789	2,028	2,387	75	27	18	0.62	0.22	0.55	0.17	0.14	0.06	22.00	3.60	14.14	2.15
MS04	13	3,023	1,039	1,773	100	20	43	0.76	0.27	0.52	0.13	0.09	0.05	22.96	2.65	14.43	3.05
MS05	9	2,616	1,004	1,817	70	12	30	0.91	0.28	0.69	0.13	0.12	0.07	25.26	3.38	12.87	2.18
MS06	10	3,017	1,532	2,230	80	23	31	0.76	0.20	0.56	0.11	0.10	0.04	23.64	2.98	14.56	2.04
MS07	3	2,315	2,169	2,254	56	25	17	0.83	0.18	0.61	0.08	0.13	0.04	24.78	2.58	14.40	0.82
MS08	18	3,619	1,430	2,006	100	18	52	0.70	0.18	0.55	0.09	0.10	0.04	22.67	2.55	13.96	2.39
MS09	12	4,264	1,170	1,764	80	22	33	0.71	0.15	0.66	0.22	0.12	0.14	23.11	2.06	13.30	3.15
All	99	4,264	1,004	1,949	105	22	310	0.73	0.23	0.58	0.15	0.11	0.07	23.08	3.05	13.89	2.74

Note: The data of sampling stations, only where enough manganese crusts were collected for chemical analysis, are used.

The average of manganese crust thickness are calculated for the average thickness in each sampling station.

S.D. means a standard deviation.

[Surface structure of manganese crusts]

[Crust]

1

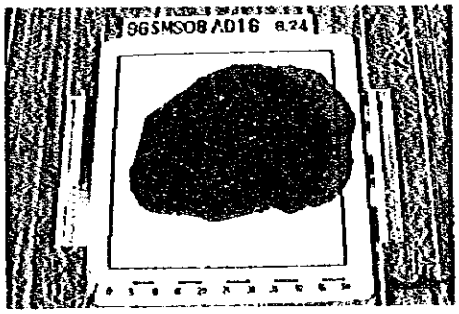

Botryoidal

5

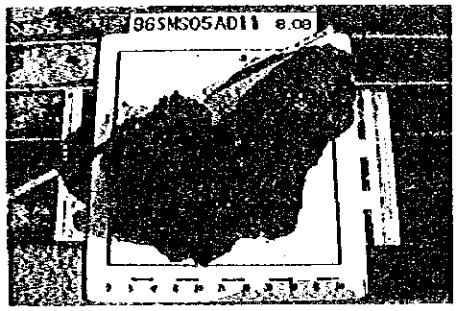

Surface

2

Stromatolite

6

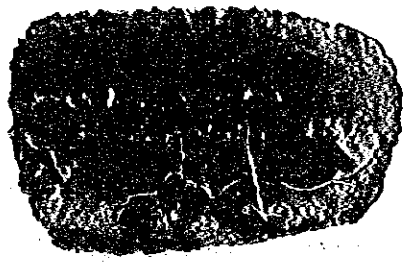

Section, three layers

3

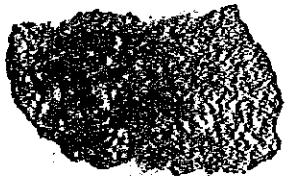

Granule

7

Section, two layers

4

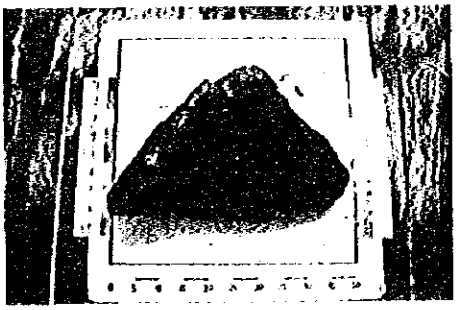

Smooth (thin coating)

8

Section, one layer

Fig. 5-3-1(1) Photographs of manganese crusts (AD sampling)

[Cobble crusts]

[Nodules]

9

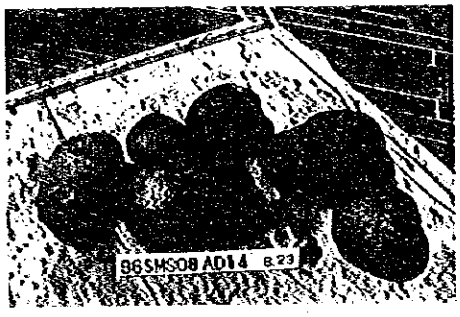

Dredged cobble crusts at a site

13

Dredged nodules at a site

10

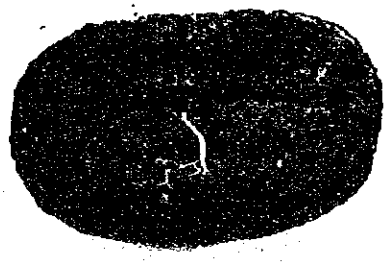

Section, three layers

14

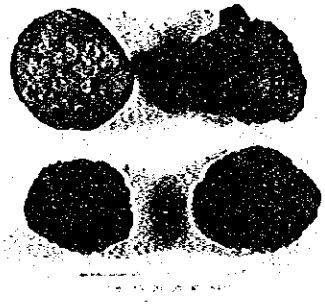

Surface

11

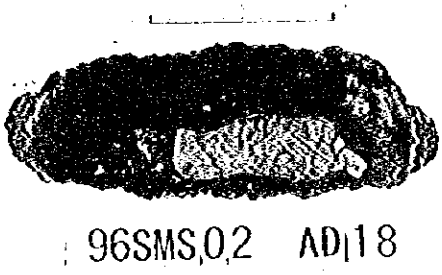

Section, two layers

15

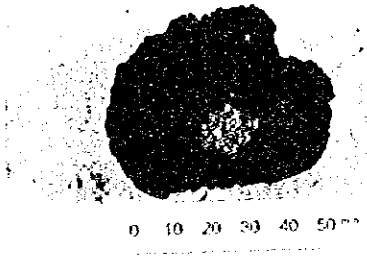

Section, two layers

12

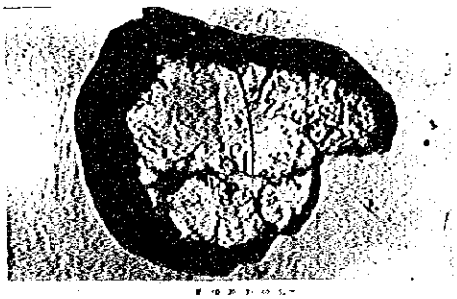

Section, one layer

16

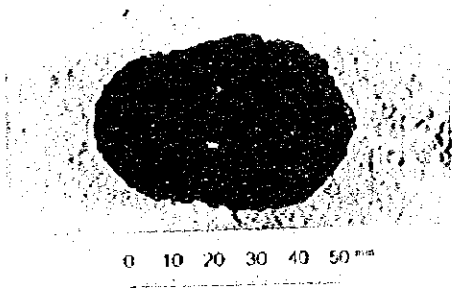

Section, no nucleus

Fig. 5-3-1(2) Photographs of manganese crusts (AD sampling)

and are divided into three layers. This indicates that the growth rate of both manganese crusts are different.

c) MS03

The average thickness of manganese crusts is 27 mm with a maximum of 75 mm. The thickest manganese crust was collected at the northern margin of the flat summit (96SMS03AD09). The crust thickness tends to be thinner at the steep uppermost flank, but this is probably caused by the efficiency of the arm dredge rather than natural features. Small amount of nodules was collected only in 96SMS03AD09 located on the flat summit.

d) MS04

The average thickness of manganese crusts is 20 mm with a maximum of 100 mm. The thickest manganese crust was collected at middle flank on the western part of seamount (96SMS04AD04). Manganese crusts with thin coating are observed throughout the seamount. There is no correlation between the crust thickness and the water depth of sampling site. Nodules were collected at many localities throughout the seamount, and particularly abundant at the ridges of the flanks.

Cobble crusts with different substrates of basalt lava, basaltic pyroclastic rocks, sandstone, and limestone were collected in 96SMS04AD09, but the nature and thickness of manganese crusts show no differences corresponding to the kinds of substrates.

e) MS05

The average thickness of manganese crusts is 12 mm with a maximum of 70 mm. The thickest manganese crust was collected at the middle flank on the southeastern side of seamount (96SMS05AD11). Manganese crusts with thin coating are observed throughout the seamount. Many thin manganese crusts with less than 5 mm thickness to thin coating were collected and thus the average crust thickness is the lowest of all seamounts surveyed. There is no clear correlation between the crust thickness and the water depth or the locality of sampling site. Nodules were collected at many localities throughout the seamount, and particularly abundant at the deeper parts of the flanks.

MS05 seamount is a peaked seamount and many basalt pebbles without manganese crusts were collected in 96SMS05AD06, 96SMS05AD07, and 96SMS05AD08 near the summit. This is believed to indicate that seafloor sediments had covered these pebbles before manganese crusts grew on them.

f) MS06

The average thickness of manganese crusts is 23 mm with a maximum of 80 mm. The thickest manganese crust was collected at upper flank on the western side of seamount (96SMS06AD02). Manganese crusts with thin coating are mainly observed on the flat summit. There is no clear

correlation between the crust thickness and the water depth or the locality of sampling site. Many nodules were collected only on the flat summit.

Only nodules were abundantly collected in 96SMS06AD07 located at the margin of the flat summit. Because the FDC observation does not show that only nodules occur widely on the flat summit, it is believed that only nodules which were easily recovered by dredge were collected under the existence of crusts in fact.

g) MS07

The average thickness of manganese crusts is 25 mm with a maximum of 56 mm. The thickest manganese crust was collected at the upper flank on the western side of seamount (96SMS07AD02). The number of sampling sites is only three, but it is the character that a large amount of nodules were collected though this is a peaked seamount.

Only nodules were collected in large amount at 96SMS07AD01. They are flat ellipsoidal in shape, the surface structure is botryoidal, the average diameter is about 5 cm, and the manganese crusts are divided into two layers with the average thickness of 15 mm.

h) MS08

The average thickness of manganese crusts is 18 mm with a maximum of 100 mm. The thickest manganese crust was collected at the flat summit margin on the northern side of seamount (96SMS08AD12). Relatively thick manganese crusts were collected at the marginal parts of the northern flat summit. There is no correlation between the crust thickness and the water depth of sampling site. Many nodules were collected on the northern flat summit.

In 96SMS08AD17 which is the deepest sampling site (3,619 m water depth), basalt boulders coated very thinly by manganese crusts were collected. On the other hand, in 96SMS08AD04 which is the shallowest sampling site (1,557 m water depth) on the flat summit margin, basalt boulders coated by manganese crusts around 1 mm thick were collected. Thus manganese crusts of thin coating occur throughout the seamount regardless of the water depth and the topography.

i) MS09

The average thickness of manganese crusts is 22 mm with a maximum of 80 mm. The thickest manganese crust was collected at the flat summit margin on the southeastern side of seamount (96SMS09AD11). There is no clear correlation between the crust thickness and the water depth or the locality of sampling site. Many nodules were collected at various localities of the seamount. The manganese crusts whose substrate is limestone tend to be relatively thin with coating thickness.

A cobble crust with 21 cm in long axis and 7 cm in height without a nucleus substrate was collected in 96SMS09AD11.

(2) Large gravity corer (LC)

LC sampling was carried out at a total of 41 sites of eight seamounts excluding MS07. These sites locate on the margin of the flat summit or around the peaked summit. The amount of manganese crusts were sufficient for shipboard chemical analysis at 23 points. Seafloor sediments were collected at 9 points as mentioned above and nothing was recovered at 11 points. The recovered materials and the seafloor photographs are listed in Table 4–2–2, and representative photographs of the manganese crusts and the seafloor are laid out in Figure 5–3–1. The results of LC sampling are summarized in Appendix Table 3 (1), (2).

1) Characteristics and occurrence of manganese crusts

The surface of the manganese crusts forms botryoidal structure (Fig. 5–3–2). The sections of sufficiently thick manganese crusts are divided into the outer and inner layers. Generally, the outer layer is compact, and the inner layer is soft and is porous sandy or thin bedded.

Manganese crusts were collected in 96SMS09LC04 and 96SMS09LC05 where seafloor sediments wholly cover the seafloor (Fig. 5–3–2, Photo Nos. 5 to 8). This fact shows that manganese crusts occur even in the areas where seafloor sediments presently cover the seafloor. This was supposed from FDC observation, and the sampling at these two localities confirmed the existence of the manganese crusts under the seafloor sediments. Rocks below the seafloor sediments were collected in 96SMS06LC05 which had the similar seafloor photograph, but manganese crusts did not occur on the rock surface (Fig. 4–2–3, Photo Nos. 7, 8). Thus, there are two types of localities where the seafloor sediments deposited before the formation of manganese crusts and where those deposited after the crusts formation. Ripple marks on the seafloor sediments are often observed on FDC observation and it is inferred that, in some cases, on the flat summits seafloor sediments move and are deposited secondarily by the current, and cover the manganese crusts.

At 10 points, except 96SMS03LC06, of the 11 points where no materials were collected, the bits of LC were damaged and it indicates the existence of manganese crusts. At six points of these 10, manganese crusts are observed in seafloor photographs (Table 4–2–2), and at three points, except 96SMS03LC04, very small amount of manganese crusts was attached to the bits. Therefore, at nine localities, excluding 96SMS03LC06 and 96SMS03LC04, although manganese crusts were not recovered, it is believed that they are exposed on the seafloor or they exist under thin sediments.

2) Occurrence of manganese crusts by seamounts

A brief description of the manganese crusts collected at each seamounts is as follows. As the LC sampling covers a very limited area and depth, it is difficult to classify the collected samples according to the classification described in 5–1 section. Therefore, in this section, manganese crusts are described without the classification except those of 96SMS02LC02 where cobble crust

was clearly identified.

a) MS01

Manganese crusts were collected at four localities in the marginal parts of the flat summit. In all cases, as no substrate was collected, it is impossible to determine the thickness of the manganese crusts. The maximum thickness, however, is more than 75 mm. The surface of the outer layer is botryoidal and the thickness of the layer is 10 to 25 mm. The outer layer is compact and the inner layer is soft and porous or compact. Some pores are filled with pale brown to yellowish white muddy materials.

Nodules were collected together with manganese crusts in 96SMS01LC05. The largest nodule is 50 mm in diameter and the nucleus of the nodule is phosphorite.

b) MS02

Manganese crusts were collected at five localities in the margin of the flat summit. In all cases, as no substrate was collected, it is impossible to determine the thickness of the manganese crusts. The thickest crust, however, is more than 60 mm thick. The surface of the outer layer is botryoidal and the thickness of the layer is 5 to 30 mm thick. The outer layer is compact, while the inner layer is soft, porous, and easily crushed to coarse sandy size by fingers. Many of the pores are filled with pale brown to yellowish white muddy materials.

Manganese crusts and cobble crusts were collected in 96SMS02LC02. The cobble crusts are over 20 mm thick and the nucleus with about 1 cm diameter is breccia consisting of manganese crust fragments.

c) MS03

Manganese crusts were collected at two localities in the margin of the flat summit. In all cases, as no substrate was collected, it is impossible to determine the thickness of the manganese crusts. The thickest crust, however, is more than 75 mm thick. The surface of the outer layer is botryoidal and the layer is 20 mm thick. The outer layer is compact, while the inner layer has thin layered structure but is soft and coarse sandy.

d) MS04

Manganese crusts were collected at one locality in the margin of the flat summit and at one locality on the middle flank of the eastern side (2,529 m water depth). At the latter site 96SMS04LC02, substrates (argillized basaltic pyroclastics) were collected, and the maximum thickness of the manganese crust is 70 mm, and the average thickness of the outer layer is 6 mm and that of the inner layer is 50 mm. The surface of the outer layer is botryoidal, and the outer layer compact and the inner layer is compact with porous to thin layered structure.

96SMS01LC05

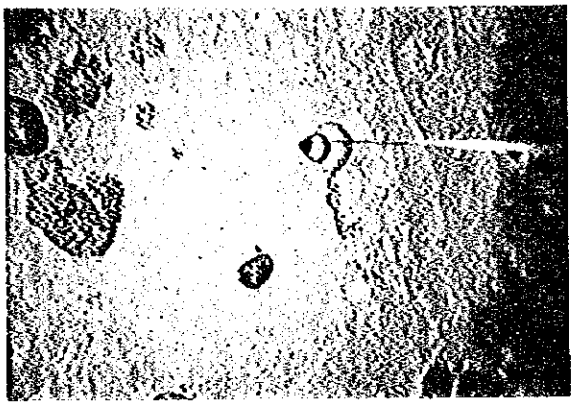

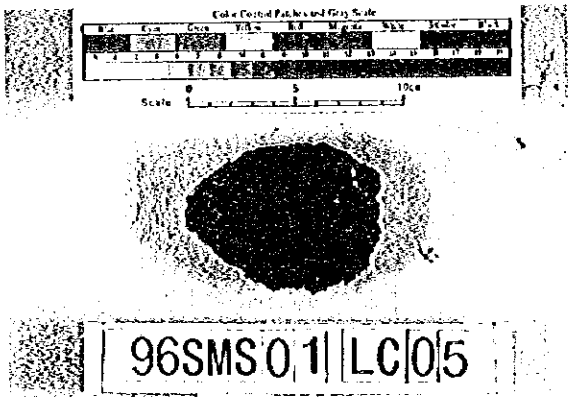

96SMS02LC04

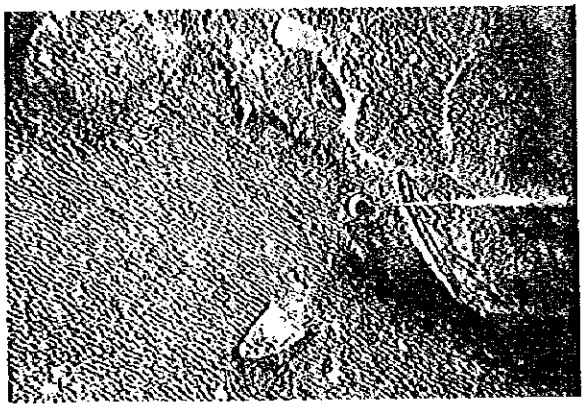

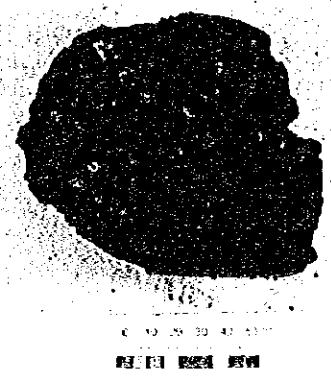

96SMS09LC04

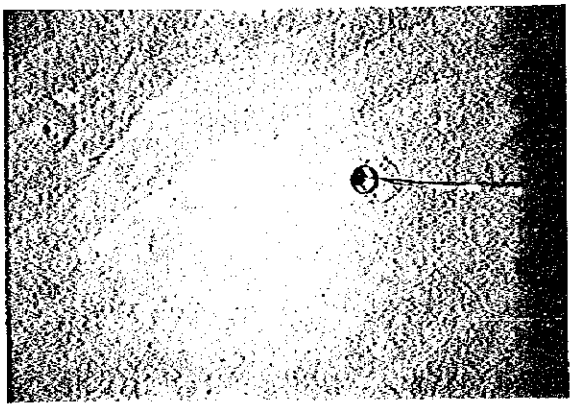

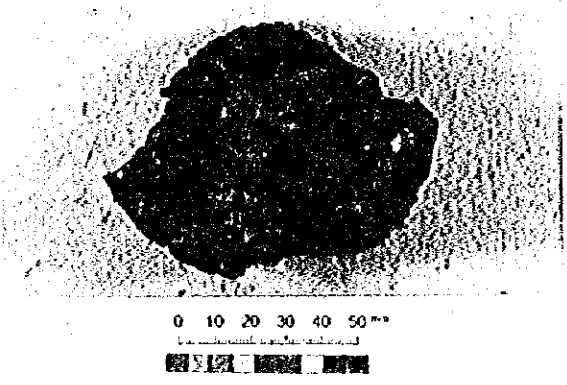

96SMS09LC05

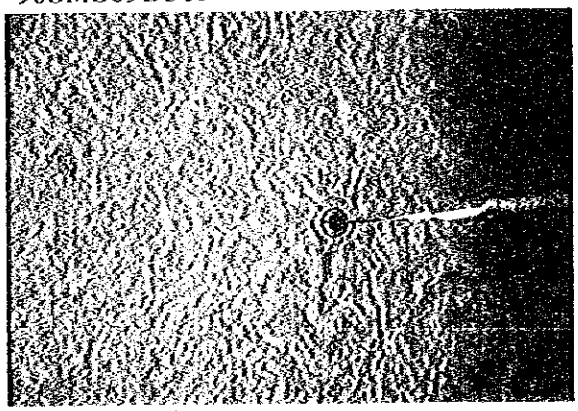

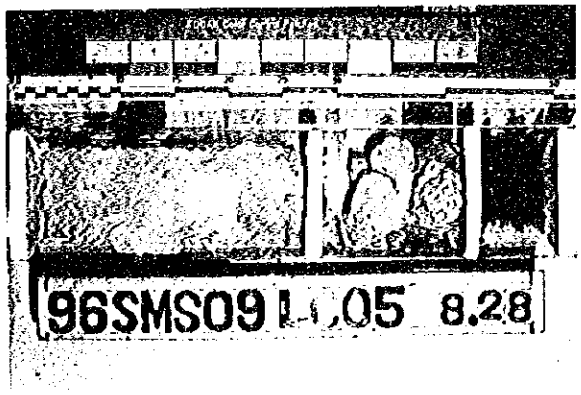

Note: In each site, upper photo shows a seafloor and lower a collected materials.

Fig. 5-3-2 Photographs of manganese crusts (LC sampling)

e) MS05

Sampling was carried out at four localities on the summit, upper flank, and foot of the peaked seamount. No manganese crusts, however, were collected at all sites. The seafloor photograph of 96SMS05LC01, located at the foot of seamount (4,651 m water depth), shows the occurrence of cobble crusts and nodules. Also, from the seafloor photographs and the deformed bits of LC, it is believed that manganese crusts occur at two localities on the summit (96SMS05LC03 and 96SMS05LC04).

f) MS06

Very small amount of manganese crusts was collected at one locality on the northern margin of the flat summit. The structure and the thickness of the manganese crust are unknown. From the seafloor photographs and the conditions of the LC bits, it is believed that manganese crusts occur at two localities in the margin of the flat summit.

g) MS08

Manganese crusts were collected at three localities on the flat summit margin and at one locality on the center of the flat summit. In all cases, as no substrate was collected, it is impossible to determine the thickness of the manganese crusts. The maximum thickness, however, is over 55 mm. The surface of the outer layer is botryoidal and the thickness of the layer is 10 to 20 mm. The outer layer is compact and the inner layer is soft and porous. Some of pores are filled with gray to yellowish white muddy materials.

Pale brown weakly consolidated foraminifera sand and manganese crusts under this sand were collected together in 96SMS08LC03.

h) MS09

Manganese crusts were collected at a total of five localities; four localities on the flat summit margin and one on the foot of seamount. The thickest crust is over 65 mm thick and the outer layer is 1 to 30 mm thick. The surface of the outer layer is botryoidal, and the outer layer is compact to porous and the inner layer is compact.

Though the seafloor photographs of 96SMS09LC04 and 96SMS09LC05 show the seafloor wholly covered by seafloor sediments, manganese crusts were collected at these two sites on the flat summit margin. At the latter site, foraminifera sand, which was 50 cm thick and covered the manganese crusts, was collected. In 96SMS09LC01 located on the southern foot of seamount (4,265 m water depth), substrates (argillized basalt lapilli tuff) accompanied by manganese crusts were collected below 15 cm thick seafloor sediments, and the average thickness of the manganese crusts is 1 mm with a maximum of 10 mm.

5-4 Chemical Composition

The manganese crusts samples were chemically analyzed for major five elements (Co, Ni, Cu, Mn, Fe) on board the survey vessel, and 26 minor elements were analyzed at a laboratory on land. The number of samples analyzed on board for the above five major elements is 310 and 119 of these samples are analyzed for minor element content. The results of the analysis are laid out in Appendix Tables 4(1) to (7).

(1) Shipboard chemical analysis for five major elements

Sampling was carried out at 78 points of AD and at 41 points of LC in all nine seamounts surveyed. Of these samples, either manganese crusts were not collected or were collected in amounts insufficient for analysis at 2 AD points and 17 LC points. Thus analysis was carried out for samples from 76 AD and 24 LC points.

For samples sufficiently thick to separate the layers of the manganese crusts, analytical samples were collected from each layer. Also when different kinds of manganese crusts or those with different substrates were collected from one AD sampling point, all types of crusts were analyzed. Therefore, several samples were analyzed at many sampling points and the number of analytical samples is 310 beside 100 sampling points.

X-ray fluorescance analysis were used on board for the five elements Co, Ni, Cu, Mn, Fe. Manganese crusts in bulk or from each layer were sampled, and about 30g of each sample were prepared for analysis in most cases, but smaller amount for samples with insufficient quantity were analyzed in some cases. After dried at 105 degrees Celsius for 24 hours and crushed, samples were prepared for analysis. Water content was also measured.

1) Characteristics of chemical composition

Manganese crusts are believed to have been formed by direct precipitation of manganese, iron and other various metals from sea water. The major components are manganese and iron hydroxides and oxides. The chemical composition varies with the location of seamounts (locality, latitude and longitude), water depth of crusts occurrence, layers of manganse crusts (related to the age and growth rate), and the kinds of manganese oxides.

Within the survey area, the chemical composition of the manganese crust varies with the seamounts or the sampling points. The ratio of the maximum and minimum content for the five elements is 3 for Mn and Fe, and 5 to 10 for Co, Ni, and Cu. These variations are caused mainly by the layers of the manganese crusts and the water depth of the sampled points. The behavior of the components to the water depth and to the crust layers is often related mutually among the five elements. This

will be reported in detail later.

The average compositions of Co, Ni, Cu, Mn, and Fe in the 310 samples are respectively 0.73, 0.58, 0.11, 23.08, and 13.89 (wt%). These values are not very different from the results of the past report in the vicinity of the Marshal Islands (Hein et al., 1988). Manganese crusts with cobalt content exceeding 0.5wt% are sometimes called cobalt-rich manganese crusts and those in the present survey area belong to this category.

In the (Co + Ni) × 10-Fe-Mn triangular diagram of Figure 5-4-1, manganese crusts of the Central Pacific are plotted somewhat to the Mn side in the center of the diagram (Hein et al., 1992). The plots of the manganese crusts from the present survey area are also concentrated in the central part of the diagram and the variation of plots is relatively small. It is of interest to note that the plots of the deep-sea manganese nodules are in an area similar to the manganese crusts in this diagram, while submarine hydrothermal manganese ores are plotted near the base line of this diagram joining Fe and Mn. The left side figures in Figure 5-4-1 are the plots of all samples analyzed, and the plots of the composition by the crust layers are shown in the right side, where cross mark shows the outer layer and black circle the inner layer.

2) Basic statistics

Basic statistical values of the five elements were calculated for each seamount, each layer of the manganese crusts, and the division of the water depth of sampling points. The results are shown in Appendix Tables 5 (1) to (5), and summarized in Table 5-3-1.

The values by seamounts show the following tendency.

* The crusts of seamount MS05 have the highest average Co, Ni, Mn content and the lowest average Fe content. And the average Mn/Fe is the highest. It is possible that this tendency is caused by seamount MS05 being a peaked seamount. Although not as pronounced, similar tendency is observed for seamount MS07 which is the another peaked seamount.

* The crusts of seamount MS03 crusts have the highest average Cu content and lowest Co and Mn average content. The average Mn/Fe value is also the lowest of the seamounts surveyed. This is considered to be the result of seamount MS03 having the deepest flat summit and a very large number of samples from the summit were analyzed. As the analytical values of the samples from the flat summit are not similar to those from the upper slopes, it is believed that the both grew under somewhat different environment.

The values by the crust layers show the following tendency.

* The average values of Co, Fe and Mn content and Mn/Fe of the outer layer are distinctly higher than those of the inner layer.

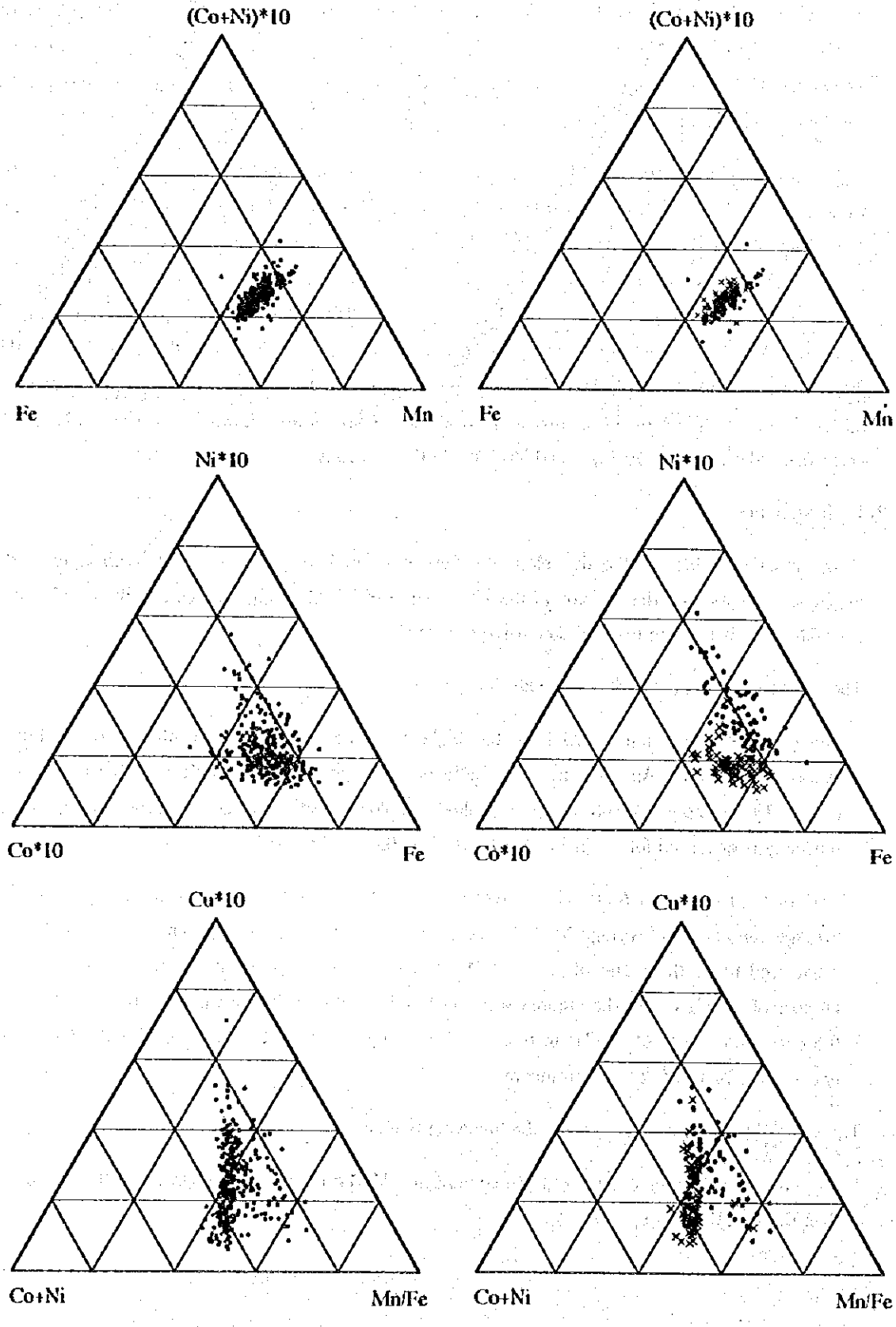

Fig. 5-4-1 Three components diagram for five major elements

* The average values of Cu and Ni content of the outer layer are higher than those of the inner layer.

The fact that the concentration of elements is different between the outer and inner layers indicate the difference of the environment and mineral formation during their growth. The two groups of elements (Co–Fe–Mn and Cu–Ni) which show the contrasting behavior of content coincide with the grouping of elements by the correlation coefficient which will be reported later.

The statistical values by the water depth of the sampling points show the following tendency. The depth grouping was done every 500 m only for the slopes and the data of the flat summit were grouped together.

* In the guyots MS01 and MS04 which have the fairly good distribution of sampling depth, the Cu and Fe average content increases with the water depth while the Ni average decreases.

* In the peaked seamount MS05, the Cu and Fe average content increases with the water depth while the Co average decreases.

* The average Co content increases with the water depth in some seamounts (MS01) and decreases in some seamounts (MS04, MS05).

* In all data of nine seamounts, the Cu and Fe average content increases and Ni average decreases with the water depth.

The variation of the average Cu, Fe, and Ni content with the water depth is harmonious with the correlation coefficients which are reported in the following section.

3) Correlation coefficients

Correlation coefficients in each seamount were calculated for the analytical results of the five elements and the water depth of the sampling points. The correlation coefficient matrixes are shown in Tables 5–4–1 (1), (2).

Some components have positive correlation for all the seamounts (for example Co–Mn), and some have either positive or negative correlation depending on the seamount (for example Co–Ni). The different behavior of the latter elements by seamounts is believed to be caused by the different topography of each seamount, the difference of the water depth range of sampling points in each seamount, and the heterogeneity of the crust layers analyzed in each seamounts. In order to minimize the effect of these heterogeneities of data and thus obtain more general correlation tendency, the correlation coefficients were examined as follows and the components with significant correlation were extracted.

Table 5-4-1(1) Correlation coefficient matrix among five major elements

Seamount: MS01

	Co	Ni	Cu	Mn	Fe	Mn/Fe	Depth
Co		-.45	-.23	.65	.54	-.34	.33
Ni			.33	.00	-.71	.70	-.38
Cu				-.05	.15	-.22	.52
Mn					.29	.07	.17
Fe						-.90	.45
Mn/Fe							-.38

Number of sample : 40

Significance level (5%) : 0.30

Seamount: MS02

	Co	Ni	Cu	Mn	Fe	Mn/Fe	Depth
Co		.29	-.29	.75	.52	-.03	-.05
Ni			.43	.48	.12	.31	-.45
Cu				-.08	-.08	.05	.11
Mn					.76	-.12	-.16
Fe						-.71	-.07
Mn/Fe							-.09

Number of sample : 46

Significance level (5%) : 0.28

Seamount: MS03

	Co	Ni	Cu	Mn	Fe	Mn/Fe	Depth
Co		.04	-.51	.69	.46	.29	.32
Ni			.68	.60	-.13	.81	-.63
Cu				.05	-.32	.40	-.43
Mn					.55	.53	-.18
Fe						-.41	.27
Mn/Fe							-.48

Number of sample : 18

Significance level (5%) : 0.43

Seamount: MS04

	Co	Ni	Cu	Mn	Fe	Mn/Fe	Depth
Co		-.11	-.75	.76	.35	-.10	-.41
Ni			-.15	.06	-.72	.86	-.55
Cu				-.33	.14	-.26	.72
Mn					.50	-.12	-.18
Fe						-.89	.51
Mn/Fe							-.60

Number of sample : 43

Significance level (5%) : 0.29

Seamount: MS05

	Co	Ni	Cu	Mn	Fe	Mn/Fe	Depth
Co		.33	-.47	.88	.20	.31	-.47
Ni			-.12	.51	-.38	.75	-.48
Cu				-.31	.40	-.52	.60
Mn					.31	.35	-.33
Fe						-.73	.64
Mn/Fe							-.74

Number of sample : 30

Significance level (5%) : 0.34

Seamount: MS06

	Co	Ni	Cu	Mn	Fe	Mn/Fe	Depth
Co		.41	-.51	.81	.32	.32	-.09
Ni			.09	.54	-.37	.83	-.60
Cu				-.20	-.06	-.06	.24
Mn					.44	.38	-.14
Fe						-.63	.42
Mn/Fe							-.44

Number of sample : 31

Significance level (5%) : 0.34

Table 5-4-1(2) Correlation coefficient matrix among five major elements

Seamount: MS07

	Co	Ni	Cu	Mn	Fe	Mn/Fe	Depth
Co		.64	-.11	.85	.28	.74	-.28
Ni			.47	.90	.10	.87	-.05
Cu				.19	-.45	.44	-.06
Mn					.30	.87	-.30
Fe						-.21	-.23
Mn/Fe							-.18

Number of sample : 17

Significance level (5%) : 0.44

Seamount: MS08

	Co	Ni	Cu	Mn	Fe	Mn/Fe	Depth
Co		-.22	-.59	.78	.72	-.42	.21
Ni			.38	.20	-.31	.55	-.34
Cu				-.27	-.29	.17	.21
Mn					.76	-.33	.11
Fe						-.86	.30
Mn/Fe							-.33

Number of sample : 52

Significance level (5%) : 0.26

Seamount: MS09

	Co	Ni	Cu	Mn	Fe	Mn/Fe	Depth
Co		-.66	-.63	.65	.68	-.56	-.40
Ni			.51	-.28	-.93	.89	.05
Cu				-.51	-.36	.17	.81
Mn					.37	-.18	-.50
Fe						-.96	.06
Mn/Fe							-.24

Number of sample : 33

Significance level (5%) : 0.33

All seamount

	Co	Ni	Cu	Mn	Fe	Mn/Fe	Depth
Co		.01	-.39	.77	.40	.00	-.09
Ni			.33	.28	-.50	.75	-.35
Cu				-.16	-.08	-.03	.45
Mn					.45	.12	-.09
Fe						-.79	.33
Mn/Fe							-.41

Number of sample : 310

Significance level (5%) : 0.11

* Combination whose correlation coefficient exceeds 5% significance level among the five major elements in more than 6 seamounts of the 9 surveyed.

Positive correlation: Co–Mn–Fe, Ni–Cu

Negative correlation: Co–Cu, Ni–Fe

* Element whose correlation coefficient with water depth exceeds 5% significance level for samples from MS01, MS04, and MS06 which have relatively homogeneous distribution of the water depth of sampling points.

Positive correlation: Water depth – Cu, water depth – Fe

Negative correlation: Water depth – Ni

The five major elements can be divided into two large groups from the correlation coefficient; Co–Mn–Fe and Ni–Cu. In the relation to the water depth, however, Cu behaves inversely with Ni, and similarly with Fe.

4) Correlation diagram

Representative correlation diagrams of the five elements and of Mn/Fe are shown in Figures 5–4–2 (1), (2). The left side figures in Figures 5–4–2 show the plots of all samples analyzed, and the right side figures those of each layer of manganese crusts (cross marks indicate the outer layer and black circles the inner layer). The chemical composition of the two layers differs considerably in thick crusts (Appendix Tables 5 (1) to (5)), and thus the data were plotted separately for the two layers. Diagrams in Figure 5–4–2 (1) show unique features when the plots of all data are compared with the those of two layers data. Mn–Co has the highest positive correlation for all data and also high positive correlation for the outer and inner layers. Mn–Ni has high positive correlation in some seamounts and it is generally weak as a whole. This combination shows weak positive correlation for all data and stronger positive value for the outer layer data. Mn–Fe has high positive correlation next to Mn–Co. It shows weak positive correlation for all data but negative correlation for the outer layer data.

Correlation diagrams for water depth and five major elements and Mn/Fe are shown in Figures 5–4–3 (1), (2). The left side figures also show the plots of all samples analyzed, and the right side figures those of each layer (cross marks indicate the outer layer and black circles the inner layer). Positive correlation for water depth–Cu and water depth–Fe, and negative correlation for water depth–Ni were extracted from the correlation coefficients, but these relations are not so clear in the diagrams. Water depth–Cu has the highest positive coefficient and it is stronger with the layer data than all data. The values for Ni, Mn, Fe and Mn/Fe varies widely in shallow part, while Cu variation is greater in deeper part.

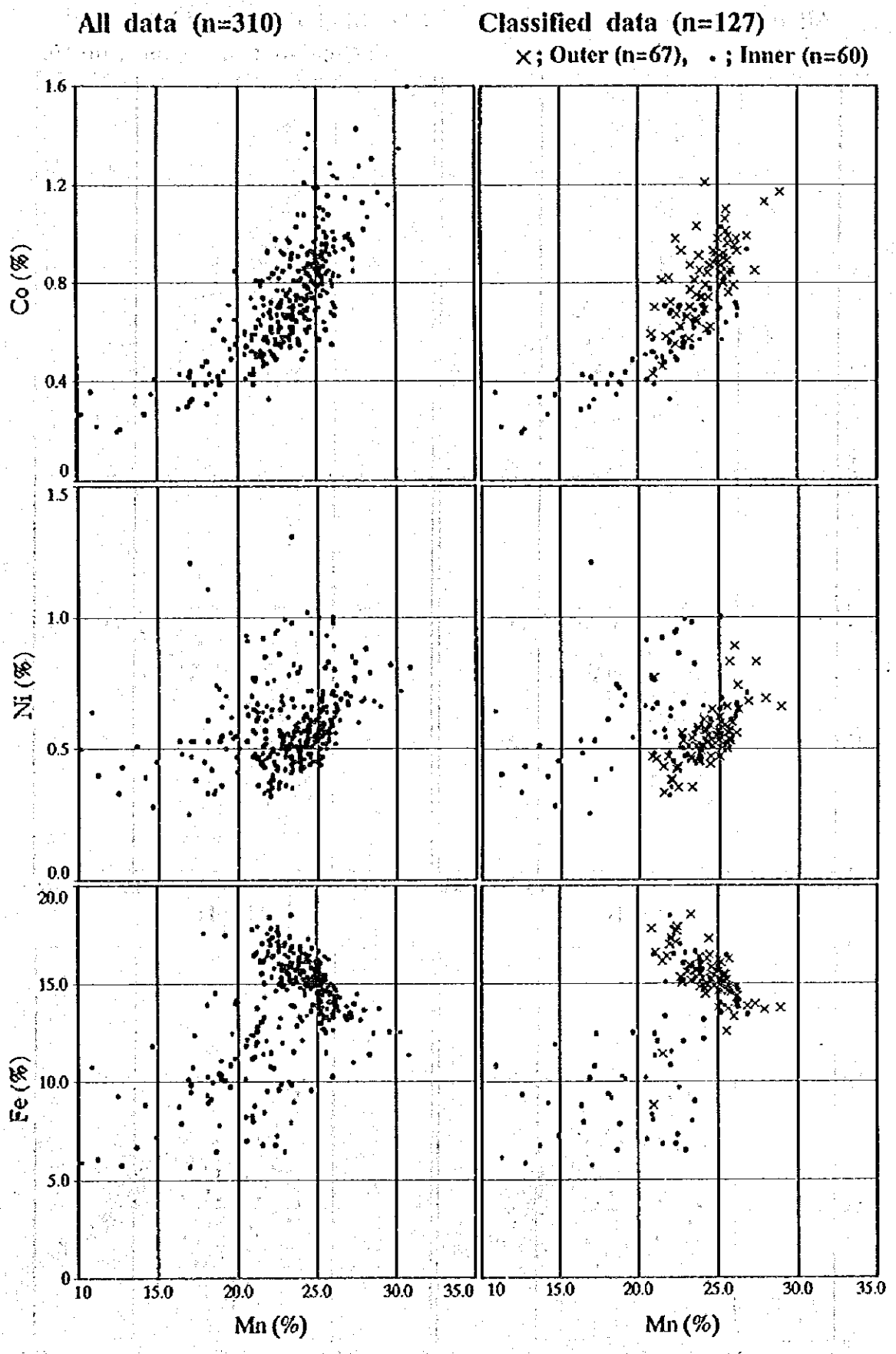

Fig. 5-4-2(1) Correlation coefficient diagram among five major elements

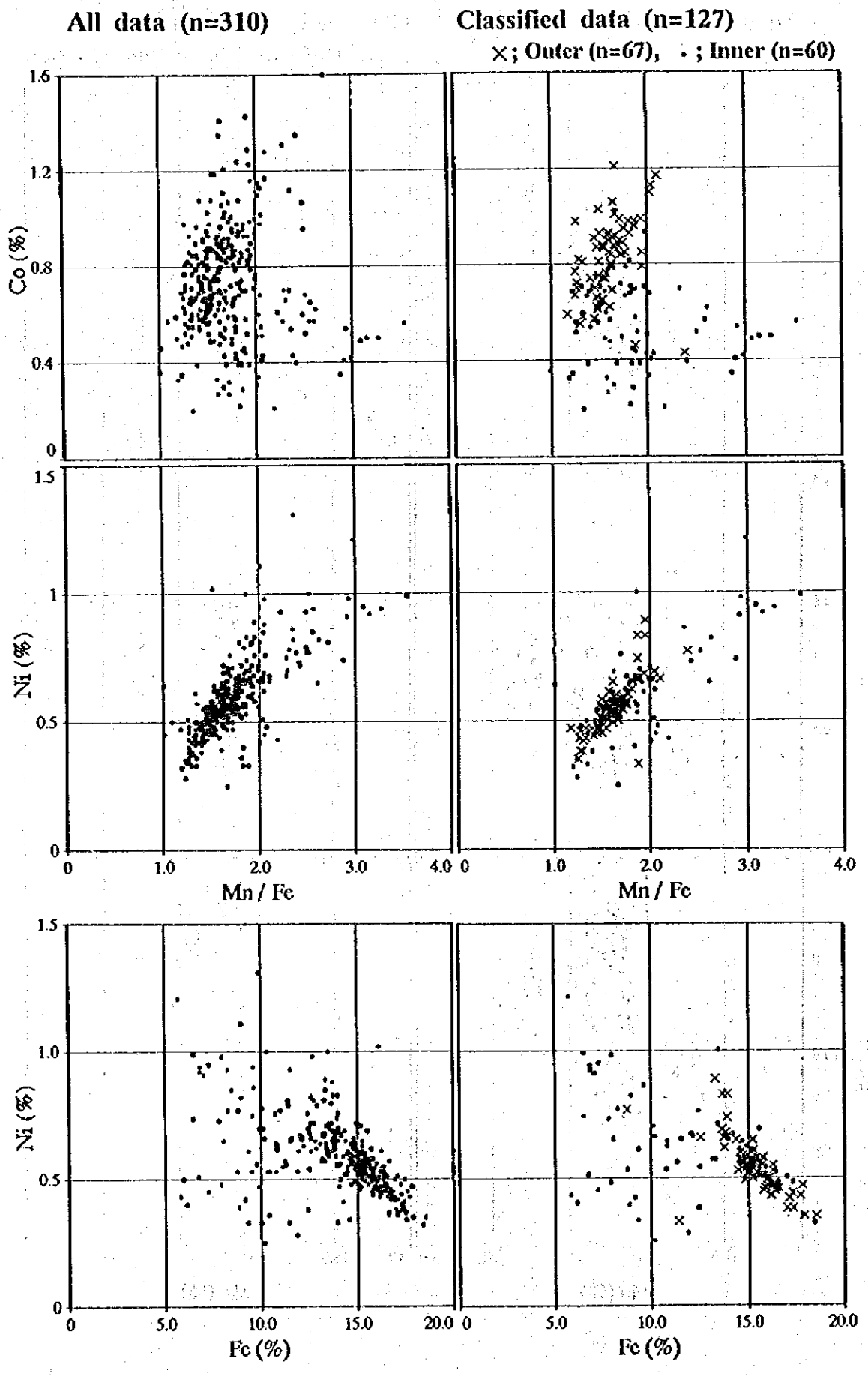

Fig. 5-4-2(2) Correlation coefficient diagram among five major elements

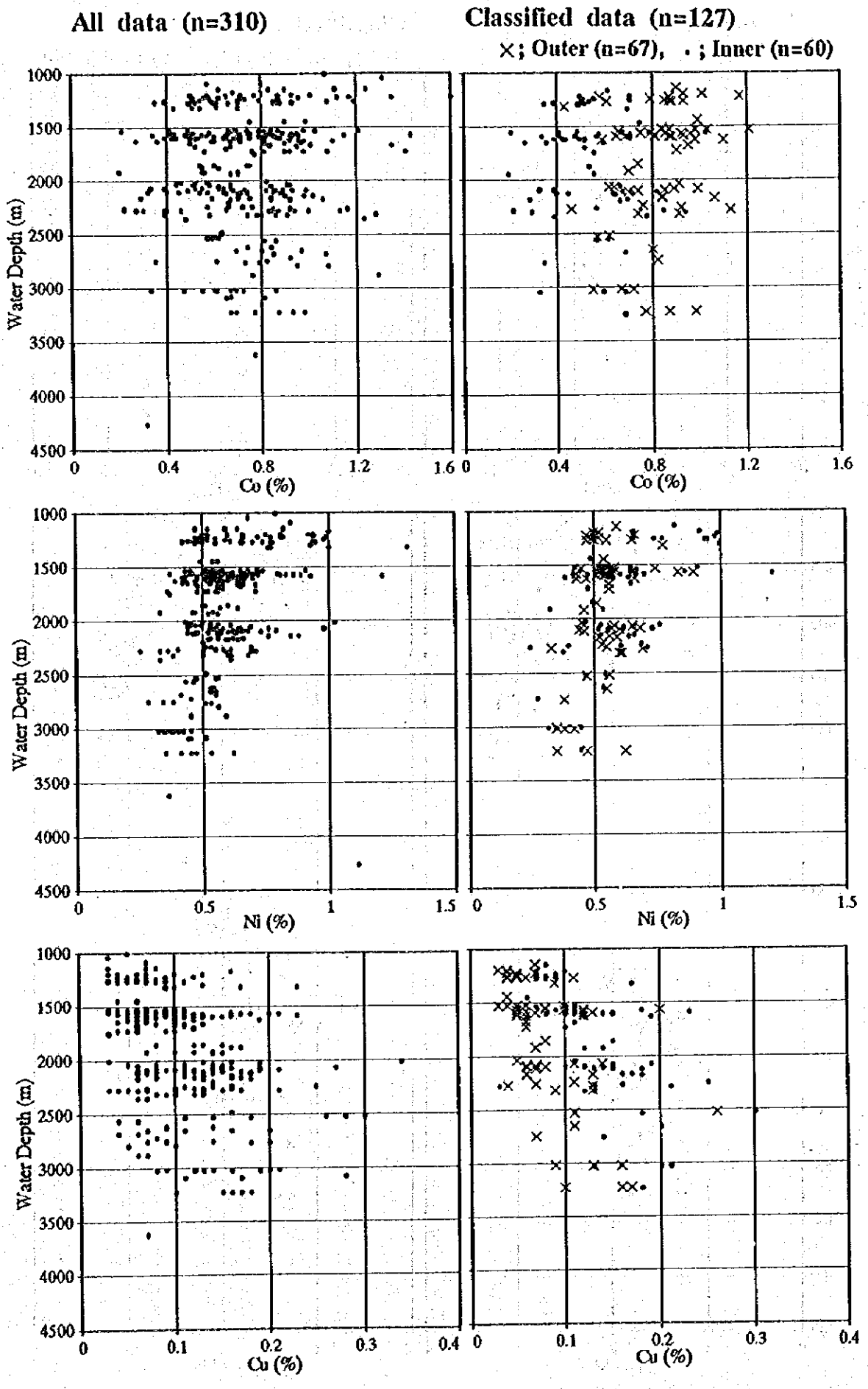

Fig. 5-4-3(1) Correlation coefficient diagram between water depth and five major elements

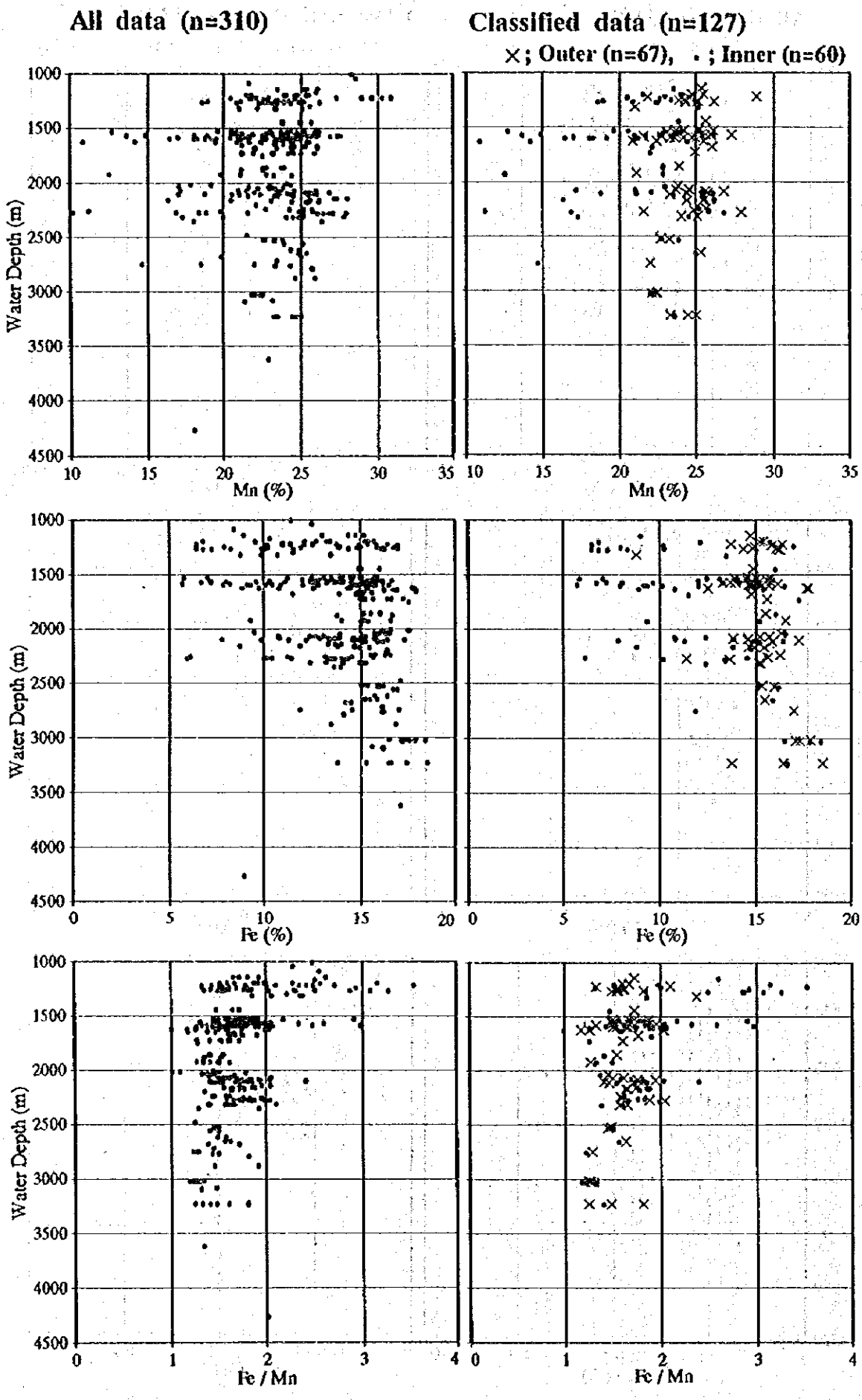

Fig. 5-4-3(2) Correlation coefficient diagram between water depth and five major elements

(2) Chemical analysis for minor elements

Of the 310 samples analyzed for the five major elements, 119 were analyzed for 26 minor elements. The analytical results are shown in Appendix Tables 4 (1) to (7).

1) Analytical methods

The methods employed and the elements analyzed are shown below. After dried until the constant weight was confirmed, the samples were prepared for analysis.

* ICP emission spectrometry: Si, Al, Ti, Ca, P, As, Ba, Pb, Zn, Mo, V, Pt

* Neutron activation analysis: La, Ce, Pr, Nd, Sm, Eu, Gd, Tb, Dy, Ho, Er, Tm, Yb, Lu

2) Analytical results

The basic statistical values are laid out in Table 5−4−2. The characteristics of the results are as follows.

* Ca content is high with a maximum of approximately 17% and an average of approximately 4.3%. This is caused by the calcareous biological remains filling the pores of the manganese crusts. Ca content tends to increase in the innermost layer.

* The maximum P content is approximately 3%, and the content tends to increase in the innermost layer. This is caused by the apatite derived from the biological remains filling the pores and forming veinlets in the innermost layer.

* Si, Al, Ti, contents tend to be low in samples with high Ca and P contents.

* Pt content tends to be higher in the inner layer than in the outer layer.

3) Correlation coefficient

Correlation coefficients were calculated for 119 samples and 34 components, namely 28 minor elements, 5 major elements, and water depth of the sampling points. The correlation matrix is laid out in Table 5−4−3. The value of 5% significance level is 0.178.

The correlations of the minor elements have the following characteristics.

* Si and Al show a very high positive correlation. Both elements show positive correlation with Ti and Fe, and negative correlation with Zn, Mo, and Ni.

* Ca and P show very high positive correlation. Both elements show negative correlation with Si, Al, Ti, As, V, Co, Mn and Fe.

Table 5-4-2 Basic statistics of minor elements

Component	Si	Al	Ti	Ca	P	As	Ba	Pb	Zn	Mo	V	Pt
Unit	%	%	%	%	%	ppm	ppm	ppm	ppm	ppm	ppm	ppb
Maximum	8.60	1.34	1.45	17.15	2.93	666	4095	2521	814	872	816	1466
Minimum	0.50	0.06	0.40	1.91	0.10	106	908	125	387	218	326	110
Mean	2.74	0.32	0.88	4.31	0.49	201	1661	937	542	515	534	415
Standard deviation	1.286	0.017	0.114	0.910	0.156	53.0	29.0	311.8	10.6	79.3	27.6	84.9
Number of sample	119	119	119	119	119	119	119	119	119	119	119	119

Component	La	Ce	Pr	Nd	Sm	Eu	Gd	Tb	Dy	Ho	Er	Tm	Yb	Lu
Unit	ppm	ppm	ppm	ppm	ppm	ppm	ppm	ppm	ppm	ppm	ppm	ppm	ppm	ppm
Maximum	393.6	1533.9	56.6	257.2	56.1	13.6	59.2	9.1	56.7	13.9	44.7	6.0	40.9	7.1
Minimum	147.2	495.3	19.0	84.5	18.9	4.9	24.4	3.6	24.1	5.3	17.1	2.5	16.3	2.8
Mean	228.2	769.6	32.9	146.5	32.1	8.1	36.8	5.7	35.8	7.7	24.1	3.4	23.2	3.8
Standard deviation	15.06	14.99	4.43	18.03	4.03	0.93	0.64	0.49	2.05	0.14	0.14	0.01	0.49	0.23
Number of sample	119	119	119	119	119	119	119	119	119	119	119	119	119	119

Table 5-4-3 Correlation coefficient matrix among five major elements and minor elements

	Si	Al	Ti	Ca	P	As	Ba	Pb	Zn	Mo	V	Pt	La	Ce	Pr	Nd	Sm	Eu	Gd	Tb	Dy	Ho	Er	Tm	Yb	Lu	Co	Ni	Cu	Mn	Fe	WD
Si	1																															
Al	.91	1																														
Ti	.46	.33	1																													
Ca	-.55	-.37	-.69	1																												
P	-.52	-.35	-.71	.99	1																											
As	.15	.03	.13	-.44	-.41	1																										
Ba	-.17	-.05	.13	.19	.17	-.23	1																									
Pb	.05	-.01	.06	-.25	-.22	.33	-.15	1																								
Zn	-.47	-.26	-.21	.25	.23	-.30	.41	-.19	1																							
Mo	-.50	-.51	-.25	-.14	-.15	.27	.07	.32	.36	1																						
V	-.01	-.09	.13	-.47	-.47	.47	.18	.28	-.03	.64	1																					
Pt	-.40	-.22	.01	.34	.32	-.28	.30	-.06	.46	-.12	-.32	1																				
La	.00	-.06	.09	.25	.26	-.05	.25	-.03	-.19	-.24	-.03	.07	1																			
Ce	-.23	-.23	.27	.14	.13	-.06	.56	.08	.15	.09	.20	.37	.51	1																		
Pr	.24	.10	.37	-.12	-.10	.04	.09	-.03	-.33	-.24	.08	-.15	.86	.42	1																	
Nd	.26	.12	.32	-.10	-.08	.04	.04	-.04	-.33	-.26	.05	-.14	.85	.37	.99	1																
Sm	.31	.14	.40	-.20	-.18	.09	-.03	.00	-.39	-.26	.07	-.22	.80	.32	.98	.97	1															
Eu	.29	.13	.37	-.16	-.14	.08	-.04	.00	-.39	-.27	.04	-.20	.82	.32	.98	.97	.99	1														
Gd	.16	.05	.24	.04	.06	.01	.09	.01	-.27	-.25	-.02	-.02	.92	.50	.95	.95	.93	.94	1													
Tb	.23	.07	.28	-.07	-.05	.07	-.06	.01	-.38	-.27	-.01	-.16	.87	.31	.97	.96	.98	.99	.96	1												
Dy	.17	.04	.17	.03	.05	.06	-.07	.02	-.34	-.26	-.06	-.09	.90	.30	.92	.93	.92	.95	.96	.98	1											
Ho	.05	-.03	-.03	.23	.25	-.01	-.06	.00	-.26	-.27	-.16	.04	.92	.28	.81	.84	.79	.82	.90	.90	.96	1										
Er	-.02	-.07	-.12	.31	.32	-.01	-.06	.01	-.21	-.23	-.18	.09	.89	.26	.73	.76	.70	.74	.85	.83	.91	.99	1									
Tm	.00	-.07	-.09	.27	.28	.02	-.10	.02	-.24	-.23	-.16	.08	.87	.24	.72	.76	.69	.74	.83	.82	.91	.98	.99	1								
Yb	.03	-.03	-.07	.26	.28	.01	-.10	.01	-.24	-.27	-.19	.09	.86	.24	.72	.76	.69	.73	.83	.82	.90	.98	.99	.99	1							
Lu	-.03	-.05	-.16	.36	.38	-.02	-.07	.02	-.17	-.26	-.23	.18	.82	.23	.60	.64	.57	.62	.76	.72	.83	.94	.97	.97	.98	1						
Co	.11	-.06	.35	-.63	-.63	.47	-.40	.45	-.33	.31	.30	-.24	-.23	-.09	-.02	-.03	.06	.05	-.07	.02	-.01	-.12	-.15	-.11	-.13	-.20	1					
Ni	-.51	-.36	-.30	.15	.13	-.17	.09	-.03	.77	.49	-.09	.37	-.37	-.11	-.48	-.45	-.50	-.49	-.41	-.46	-.40	-.29	-.23	-.24	-.24	-.18	-.02	1				
Cu	.18	.31	.32	.00	-.02	-.35	.41	-.32	.31	-.35	-.21	.24	.06	.07	.14	.12	.11	.11	.08	.06	.02	-.02	-.05	-.06	-.02	-.02	-.45	.08	1			
Mn	.00	-.12	.42	-.75	-.76	.37	-.14	.33	.07	.53	.48	-.15	-.31	-.08	-.05	-.07	.01	-.02	-.15	-.07	-.13	-.26	-.30	-.26	-.28	-.35	.79	.28	-.16	1		
Fe	.66	.50	.55	-.77	-.75	.38	-.20	.16	-.37	-.10	.39	-.42	-.01	-.14	.30	.28	.38	.35	.16	.27	.18	.00	-.08	-.06	-.05	-.14	.38	-.45	.04	.46	1	
WD	.42	.32	.61	-.25	-.26	-.15	.20	-.24	-.21	-.45	-.10	-.23	.42	.24	.64	.59	.65	.64	.52	.58	.48	.31	.22	.22	.24	.14	-.10	-.44	.55	-.04	.40	1

note n=119

WD: Water depth

* Pt show positive correlation with Ca, P, Ba, Zn and Ni, and negative correlation with Si, V and Fe.

* REE mutually show high positive correlation. REE show negative correlation with Zn, Mo, Ni. The light REE show positive correlation with Si and Ti, while the heavy REE with Ca and P.

As mentioned previously, the five major elements were divided into two groups Co–Mn–Fe and Ni–Cu. The correlation between these groups and the minor elements are as follows.

* Co–Mn–Fe combination has positive correlation with Ti, As, Pb and V, and negative correlation with Ca and P.

* Ni–Cu has positive correlation with Zn and Pt.

The water depth has positive correlation with Si, Al, Ti and REE, and negative correlation with Mo.

4) Factor analysis

Factor analysis, one of the multivariate analysis, was conducted for 34 components of the 119 samples whose correlation coefficients were calculated. The communality is estimated from the multiple correlation coefficients. Factor loadings and factor scores are calculated after normal varimax rotation. The number of factors is decided as five from the eigenvalues and cumulative contributions. The factor loading values are shown in Table 5–4–4.

The characteristics of the five factors are as follows.

a) First factor

The 13 REE components, excluding Ce, have factor loadings exceeding 0.87, and there is no other component with higher factor loading values. The reason for the high contribution of only REE to the first factor is that REE occupy 14 of the 34 components and also that they mutually have a very high positive correlation coefficient. Other than REE, the water depth has low positive contribution. Therefore, the first factor expresses the behavior of REE with a small contribution of the water depth. Regarding correlation coefficients, light REE have higher positive correlation with the water depth than the heavy REE.

Two samples, each from seamounts MS01 and MS03, have factor scores higher than mean value (M) + 2 × standard deviation (SD), but no geologic features common to these samples are observed. No samples from either MS05 and MS08 have factor scores higher than M+SD, while many have those below M–SD.

Table 5-4-4 Results of factor analysis

Component name	Factor loadings (after varimax rotation)				
	First factor	Second factor	Third factor	Fourth factor	Fifth factor
Si	0.070	-0.558	0.316	-0.598	-0.249
Al	-0.039	-0.440	0.468	-0.461	-0.231
Ti	0.123	-0.825	0.146	-0.080	0.231
Ca	0.107	0.910	0.298	0.174	0.071
P	0.123	0.914	0.286	0.140	0.049
As	0.030	-0.233	-0.542	-0.228	-0.093
Ba	-0.043	0.048	0.262	0.199	0.758
Pb	0.026	-0.120	-0.479	-0.034	-0.090
Zn	-0.268	0.103	0.154	0.741	0.265
Mo	-0.234	0.039	-0.758	0.338	0.244
V	-0.096	-0.259	-0.652	-0.174	0.446
Pt	0.025	0.167	0.286	0.641	0.097
La	0.919	0.143	0.080	-0.069	0.279
Ce	0.350	0.036	-0.040	0.164	0.734
Pr	0.888	-0.239	0.053	-0.207	0.272
Nd	0.904	-0.213	0.055	-0.192	0.191
Sm	0.871	-0.310	0.024	-0.247	0.164
Eu	0.899	-0.274	0.031	-0.235	0.136
Gd	0.951	-0.082	0.056	-0.109	0.206
Tb	0.950	-0.171	0.014	-0.188	0.079
Dy	0.985	-0.066	0.008	-0.117	0.004
Ho	0.980	0.142	0.039	-0.011	-0.078
Er	0.951	0.233	0.022	0.044	-0.119
Tm	0.949	0.203	-0.003	0.036	-0.151
Yb	0.945	0.185	0.043	0.037	-0.162
Lu	0.885	0.287	0.072	0.088	-0.185
Co	-0.033	-0.505	-0.645	-0.007	-0.276
Ni	-0.314	0.089	-0.086	0.824	-0.098
Cu	0.012	-0.290	0.701	0.201	0.255
Mn	-0.141	-0.692	-0.582	0.288	-0.047
Fe	0.084	-0.725	-0.127	-0.431	-0.059
Water depth	0.406	-0.486	0.459	-0.247	0.304

b) Second factor

Ca and P have factor loadings higher than 0.9, and Ti, Mn and Fe have those less than −0.69, and these components contribute most highly to the second factor. Si, Al and Co have factor loadings below −0.44, but they have larger values to other factors. The second factor indicate the amount of biological remains. The fissures and voids of the manganese crusts are filled with biological remains and apatite derived therefrom, and the increase of these material indicates the decrease of the major components of the manganese crusts, namely manganese and iron.

Most of the samples with factor score exceeding M+2 × SD are from the innermost layer of the crusts. This is caused by the fact that the fissures and voids of the innermost layer are often completely filled with apatite and that apatite veinlets occur.

c) Third factor

The factor score of Cu is 0.7, Al 0.46, Mo, V, As, Pb and Co range from −0.47 to −0.75. These components have the highest contribution to the third factor. The water depth shows positive contribution and Mn shows negative contribution, but they contribute more largly to other factors. The third factor indicates the enrichment of Cu, and of heavy metals as Mo, V, Pb, and Co, which show inverse correlation to Cu. The water depth also contributes to this factor.

Samples with factor scores greater than M+SD are mostly from the inner or innermost layer of the crusts. All samples with factor score less than M−2 × SD occur in shallow water depth between 1,200 and 1,300m.

d) Fourth factor

Zn, Pt, and Ni have factor score of 0.64 to 0.82, and Si has −0.60, and these components have the highest contribution to the fourth factor. Al and Fe show negative contribution, but they contribute more largly to other factors. The fourth factor indicates the enrichment of Zn, Pt, and Ni.

Each two samples, from seamounts MS01 and MS09, have factor scores higher than M+2 × SD, but the common geologic features are not recognized among these samples. Many samples from seamount MS04 have factor scores below M−SD.

e) Fifth factor

Ba and Ce have factor scores higher than 0.73, and these components have the highest contribution to the fifth factor. The fifth factor indicates the enrichment of Ba and Ce.

No common geologic features are observed among samples with factor scores above M+SD.

Among the major five elements, Cu and Ni belong to the same group, and have inverse correlation with the Co−Mn−Fe group. From factor analysis, however, the two elements are

divided into different factors. Cu contributes to the third factor and has inverse correlation with Co and Mn. On the other hand, Ni contributes to the fourth factor, and has no relation with the other four components.

5-5 Mineral Composition

The main constituents of manganese crusts are manganese and iron oxides. The kinds of manganese oxides which occur on the seafloor differs by the form (crusts, nodules, chimneys, etc.) and their genetic environment (seamounts, deep seafloor, volcanoes, etc.). The deposition of manganese crusts are considered to be of hydrogenetic origin and the manganese mineral is vernadite (δ -MnO_2) (Usui, 1996).

(1) Microscopic observation of polished section

Polished sections were prepared for the manganese crusts collected by AD sampling and were studied by reflection microscope. The total number of samples studied was 21, one to three samples from each seamount. X-ray diffractometry was carried out for these 21 samples. The results of microscopic study are laid out in Table 5-5-1, and representative microphotographs are shown in Figure 5-5-1.

Vernadite, todorokite, iron hydroxide, and collophane were identified. In the 21 samples studied, vernadite is the main constituent mineral and it comprises 80 to 90 % of the manganese crusts. Iron hydroxide and collophane occur in many samples in minor amount. Todorokite is identified in two samples, namely 96SMS01AD08-P1 and 96SMS05AD06-P1. Low reflectivity materials fill the space of granular vernadite and they are supposed to be apatite by X-ray diffractometry.

Vernadite occurs in various shapes and textures, and they are largely grouped into banded to stratiform, long columnar, and colloform to granular. Banded texture tends to be developed in the inner and innermost layers of manganese crusts, and columnar to colloform texture in the outer layer. The width of the growth bands is 0.01 to 0.05 mm.

Manganese crusts almost totally consists of one manganese mineral, vernadite. It means that no difference of minerals by the types of manganese crusts (crusts, cobble crusts, and nodules) and by the layer of the crusts (outer, inner, and innermost) exist. The texture of the mineral varies considerably and there is a relationship between the mineral texture and the crust layers.

Table 5-5-1 Results of microscopic observation for manganese crusts polishes

Sampling point No.	Code No.	Texture-structure	Forming Minerals					Remarks
			Vernadite	Todorokite	Iron hydroxide	Collophane	Silicate minerals	
96SMS01 AD08	P1	sheet~concretion	◎	○	+			tinyvein network of iron hydroxite
96SMS01 AD10	P1	colloform, ellipse	◎		+			tinyvein network of iron hydroxite
96SMS01 AD12	P1	concretion, spherical	◎		+	+		tinyvein network of iron hydroxite
96SMS02 AD07	P1	colloform~spherical, ellipse	◎		+			tinyvein of iron hydroxite in spherical structure
96SMS02 AD07	P2	colloform, spherical	◎		+	+		tinyvein of iron hydroxite and collophane
96SMS02 AD13	P1	banded, spherical	◎		+	+		tinyvein of collophane and iron hydroxide
96SMS03 AD09	P1	spherical, columnar~colloform, concretion, ellipse	◎		+	+	?	tinyvein of iron hydroxite and silicate minerals (?)
96SMS03 AD09	P2	colloform~spherical, concretion, sheet~concentric circle	◎		+	+		tinyvein of iron hydroxite
96SMS04 AD04	P1	colloform~columar, ellipse	◎					
96SMS04 AD04	P2	columar, concretion	◎		+			
96SMS04 AD12	P1	colloform, columar, spherical, sheet	◎		+	+		tinyvein network of collophane and iron hydroxide
96SMS05 AD06	P1	concretion, columar, colloform	◎	+				
96SMS06 AD02	P1	colloform~concretion, ellipse	◎					tinyvein of low reflective power minerals
96SMS06 AD02	P2	colloform, radial	◎		+	+		tinyvein of iron hydroxite
96SMS06 AD12	P1	colloform, spherical, grain, ellipse	◎		+	+		tinyvein of iron hydroxite in spherical structure
96SMS07 AD01	P1	spherical, concretion, ellipse	◎		+	+		tinyvein of iron hydroxide and iron hydroxide
96SMS08 AD12	P1	colloform, grain, columar, unsettled form	◎			+		tinyvein of collophane
96SMS08 AD12	P2	sheet~colloform	◎			+		
96SMS09 AD08	P1	colloform, grain~spherical~unsettled form	◎		+			tinyvein of iron hydroxite
96SMS09 AD11	P1	concretion, colloform	◎					
96SMS09 AD11	P2	ellipse	◎			+		tinyvein of low reflective power minerals

Legend ◎ : Abundant ○ : Common + : Few~Rare ? : Uncertain

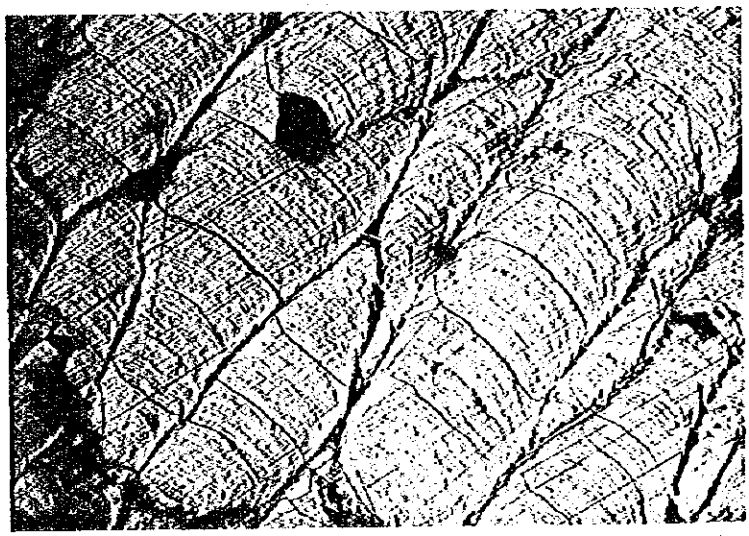

96SMS04AD04P1
Outer layer,
columnar texture

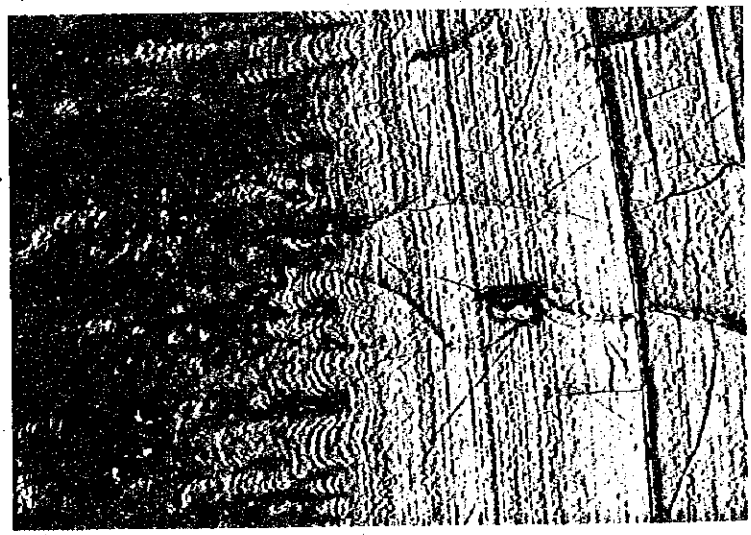

96SMS08AD12P2
Innermost layer,
columnar texture
and banded texture.

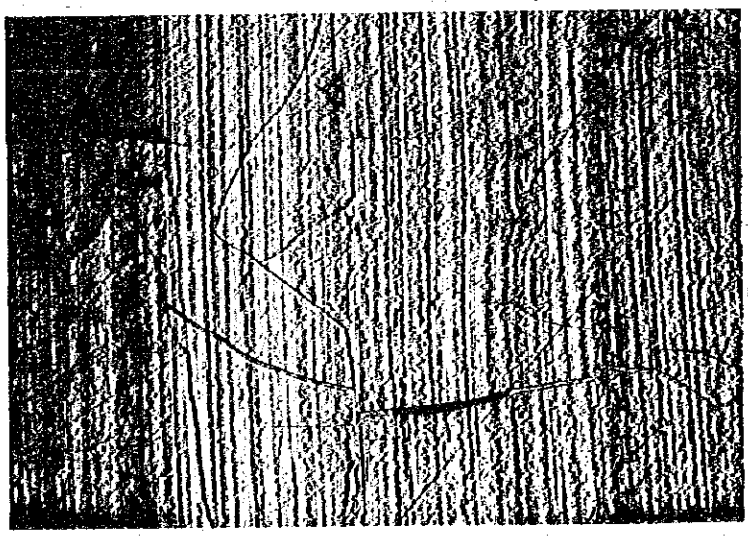

96SMS08AD12P2
Innermost layer,
banded texture

Fig. 5-5-1 Photographs of microscopic observation of manganese crusts polishes

(2) X-ray diffraction analysis

The 21 microscopically studied samples were examined by X-ray diffractometry. Powder and non-orientation specimens were measured. The results are shown in Table 5-5-2.

Identified minerals are vernadite, todorokite, birnessite, quartz, feldspar, and apatite.

A large amount of vernadite was detected in all 21 samples, and a small amount of todorokite and birnessite were detected in several samples. These manganese minerals have wide diffraction peaks and are considered to be poorly crystallized. Vernadite has only two diffraction peaks, and this is also called two-peaked δ -MnO_2

Apatite occurs filling voids and forming veinlets as observed by unaided eyes. Small to medium amount of apatitre are found in many samples. Quartz and apatite are considered to have been derived from biological remains such as diatoms and foraminifera, and feldspars from volcanic rocks.

5-6 Growth Rate

Concentration of 10Be was measured in order to determine the growth rate of manganese crusts. Five samples were studied and two to three points of different depth were measured for each sample. The results are shown in Table 5-6-1.

The samples were, after grinding, dried at 120 degrees Celcius for 12 hours and the constant weight was confirmed. 500 micrograms of 9Be was added as carrier to 500 mg of sample. Tandem accelerator and accelerator mass spectrometer were used for the measurement of 10Be.

The growth rate of manganese crusts is estimated with the assumption that the 10Be concentration in sea water is constant and that its behavior does not change during deposition. As the 10Be concentration increases from the deep part to the surface of manganese crusts, the growth rate is calculated from the diagram of the measured depth and 10Be concentration. In 96SMS06AD02, the growth rate was not calculated because of the reverse relation between the depth and the concentration.

The growth rate is 2.6 to 5.2 mm/Ma with the average of 3.6 mm/Ma. Thus 10 cm thick manganese crust grew to the present state during a period of 28 million years. Since the seamounts on which manganese crusts occurred were formed in Late Cretaceous, this growth rate is a reasonable value. Also Sharma and Somauajulu (1982) reported that the growth rate of manganese crusts in the Pacific region was one to eight mm/Ma.

Table 5-5-2 Results of X-ray diffraction analysis for manganese crusts

Sampling point No.	Code No.	Manganese crust		Mn-hydroxide			Others			Chemical analysis code No.
		Crust Type	Analized portion	Vernadite	Todorokite	Birnessite	Quartz	Feldspar	Apatite	
96SMS01 AD08	X1	crust	bulk	◎	?				○	AA
96SMS01 AD10	X1	crust	bulk	◎			+			AA
96SMS01 AD12	X1	pebble	surface (inner)	◎		?			○	A2
96SMS02 AD07	X1	crust	outer	◎			+			A1
96SMS02 AD07	X2	crust	innermost	◎					○	A3
96SMS02 AD13	X1	pebble	surface (outer)	◎					○	A1
96SMS03 AD09	X1	crust	outer	◎			+		+	B1
96SMS03 AD09	X2	crust	inner	◎					○	B2
96SMS04 AD04	X1	crust	outer	◎			+			A1
96SMS04 AD04	X2	crust	inner	◎			+			A2
96SMS04 AD12	X1	pebble	innermost	◎					○	A4
96SMS05 AD06	X1	pebble	surface (bulk)	◎					+	AA
96SMS06 AD02	X1	crust	outer	◎			+			A1
96SMS06 AD02	X2	crust	innermost	◎					○	A3
96SMS06 AD12	X1	crust	outer	◎			+	+		A1
96SMS07 AD01	X1	nodule	bulk	◎			+		+	BB
96SMS08 AD12	X3	pebble	outer	◎					○	–
96SMS08 AD12	X4	pebble	innermost	◎					+	–
96SMS09 AD08	X1	crust	bulk	◎			+			AA
96SMS09 AD11	X1	crust	outer	◎			+			A1
96SMS09 AD11	X2	pebble	innermost	◎		?	+		○	B3

Legend ◎ : Abundant ○ : Common + : Few~Rare ? : Uncertain

Table 5-6-1 Results of isotopic analysis for 10Be of manganese crusts

Sampling point No.	Code	Depth (mm)	Type and layer of sample	10Be content (dpm/kg)	Growth rate (mm/Ma)
96SMS01AD11	B1	0	Cobble crust, outer layer	25.469	3.4
96SMS01AD11	B1	22	ditto	2.092	
96SMS01AD11	B2	50	Cobble crust, inner layer	1.78	
96SMS06AD02	B2	30	Crust, inner layer	0.040	reverse
96SMS06AD02	B3	50	Crust, innermost layer	0.053	
96SMS07AD02	B1	0	Crust, outer layer	10.732	5.2
96SMS07AD02	B2	30	Crust, inner layer	1.179	
96SMS08AD12	B1	20	Crust, outer layer	8.269	3.4
96SMS08AD12	B1	30	ditto	1.178	
96SMS08AD12	B2	70	Crust, innermost layer	0.052	
96SMS09AD11	B1	0	Crust, outer layer	30.8	2.6
96SMS09AD11	B1	18	ditto	2.74	
96SMS09AD11	B2	35	Crust, innermost layer	0.963	

Table 5-7-1 Results of lead isotope analysis for manganese crusts

Sampling point No.	Code	Sample contents		206Pb/204Pb	207Pb/204Pb	208Pb/204Pb
		Crust type	Layer			
96SMS01AD11	IS1	Cobble crust	Outer layer	18.720	15.662	38.861
96SMS01AD11	IS2	Cobble crust	Inner layer	18.648	15.648	38.771
96SMS02AD07	IS1	Crust	Outer layer	18.706	15.645	38.799
96SMS02AD07	IS2	Crust	Inner layer	18.673	15.654	38.768
96SMS04AD04	IS1	Crust	Outer layer	18.737	15.714	39.039
96SMS04AD04	IS2	Crust	Inner layer	18.647	15.657	38.828
96SMS05AD11	IS1	Crust	Outer layer	18.709	15.641	38.783
96SMS05AD11	IS2	Crust	Inner layer	18.673	15.641	38.726
96SMS06AD02	IS1	Crust	Outer layer	18.705	15.649	38.809
96SMS06FD01	IS1	Crust	Outer layer	18.784	15.741	39.090
96SMS06FD01	IS2	Crust	Inner most layer	18.653	15.636	38.699
96SMS08AD12	IS1	Cobble crust	Outer layer outer	18.738	15.682	38.911
96SMS08AD12	IS2	Cobble crust	Outer layer inner	18.637	15.634	38.710
96SMS08AD12	IS3	Crust	Inner most layer	18.359	15.565	38.685
96SMS09AD11	IS1	Crust	Outer layer	18.714	15.660	38.856
96SMS09AD11	IS2	Crust	Inner most layer	18.688	15.661	38.832

5-7 Lead Isotopic Composition

The composition of lead isotope was measured for 16 manganese crust samples. The results of the analysis is laid out in Table 5-7-1, and the two-component diagrams of the isotope ratio in Figure 5-7-1.

(1) Analytical method

The sample was first treated by acid in order to eliminate the effect of iron oxides and biological remains, dried and the lead was extracted by Shimida and Nohdas method (1995).

Finnigan Mat mass spectrometer was used for the measurement. The measured isotope ratios are 206Pb/ 204Pb, 207Pb/ 204Pb, and 208Pb/ 204Pb. The corrections for these ratios are 1.00290, 1.00425, and 1.00628 respectively.

(2) Analytical results

The plots for all 15 samples, except for 96SMS08AD12-IS3, are fairly concentrated in Figure 5-7-1. This is in contrast to the scattered plots of the lead isotope ratios of rocks mentioned earlier.

In each sampling point (the same sample), the lead isotope ratios tend to be lower in the inner layer (code is IS2) than the outer layer (IS1). The sample 96SMS08AD12-IS3 is only of the innermost layer, and the three lead isotope ratios of this sample are the lowest and are close to the values of the general oceanic island basalt. On the other hand, the highest ratios are that of 96SMS06FD01-IS1, which are similar to those of deep ocean seafloor sediments.

Comparing the lead isotope ratios of the manganese crusts and the substrate basalt, the ratios of the basalt are higher than those of the crusts, but there is no apparent regularity. From the isotope ratios in the present, there appears to be no genetical relation between the manganese crusts and the basalt.

The fact that the high lead isotope ratios of the outer layer of manganese crusts are similar to that of the deep ocean seafloor sediments indicates that the seafloor sediments or the sea water played essential roles in the formation of the outer layer of the crusts. But the fact that the isotope ratios of the inner layer are always lower than that of the outer layer in the same crust indicates that they were not originated from seafloor sediments nor sea water alone. The study of the isotope ratio suggests that mantle-originated materials were concerned with the crust deposition at the beginning and subsequently seafloor sediments containing sea water concerned.

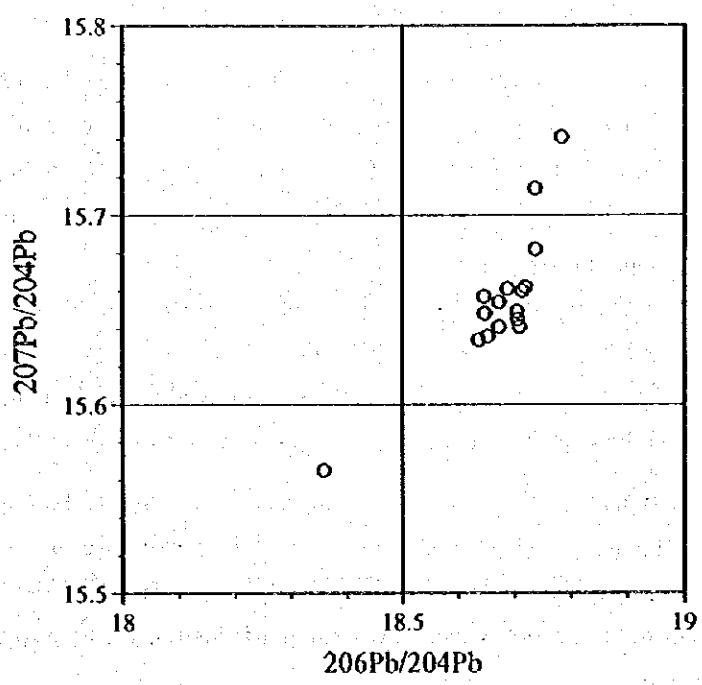

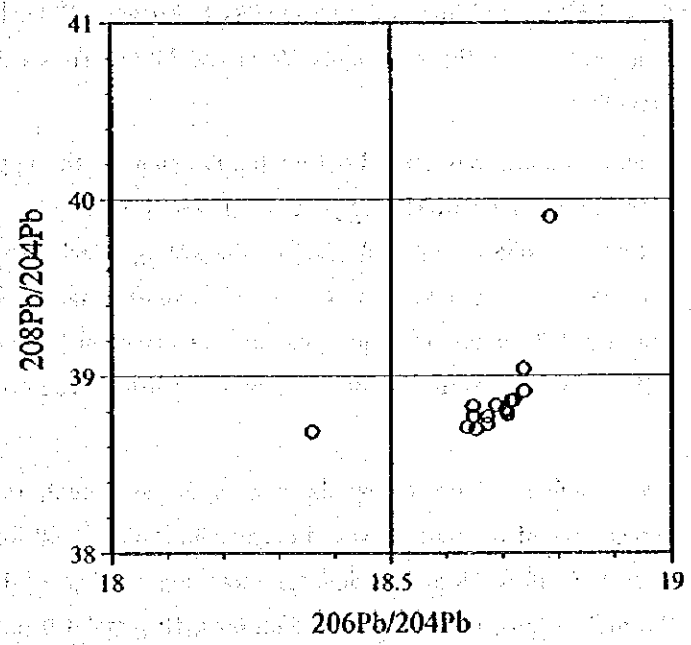

Fig. 5-7-1 208Pb/204Pb-206Pb/204Pb and 207Pb/204Pb-206Pb/204Pb diagrams

5-8 Characteristics of Occurrence

Characteristics of manganese crust deposits were investigated and the ore reserve of the manganese crusts was calculated. The values of each characteristic or the relative relations for each seamount are shown in Table 5-8-1. The factors of the characteristics are as follows; the size of the seamount, the topographic ruggedness of the seamount, the average gradient of the seamount slopes, the water depth of the seamount summit, the degree of the manganese crusts exposure, the average thickness of the crusts, Co and Pt contents, and dry reserve tonnage of the crusts. The topographic ruggedness of the seamounts was decide by bathymetric maps, and the degree of the crusts exposures by the MBES acoustic pressure figures. In other factors the actual measurements are laid out. Advantage and disadvantage characteristics as the exploitation criteria are also described together in the table.

In the margin of flat summits, manganese crusts are usually observed to be exposed continuously. In the slopes of seamounts the steeper slope tends to have the higher exposure of manganese crusts, but the steep slope and much topographic roughness are supposed to be unfavorable characteristics. On this point of view, the rugged peaked seamount without a flat summit is inferior to the guyot where manganese crusts occur on the flat summit.

Seamounts MS01, MS02, MS04, MS05, and MS07 have relatively high degree of the manganese crusts exposure, and the former three are guyots and the latter two are peaked seamounts. Co content is high in the seamounts MS05 and MS07, and low in the seamounts MS01 and MS03. Pt content is high in the seamount MS02, and somewhat low in the seamounts MS04 and MS06. Thus each seamount has an advantage and disadvantage together.

The calculation of resource volume was carried out for the flat summit, the upper and middle slope of the seamounts, excluding the lower slope which had poor manganese crusts exposures and thin crusts. The dry tonnage is calculated as the slope area is multiplied by the average thickness and the dry density of the crusts and then by a coefficient in accordance with the crust exposure ratio. The coefficient in the slope is 0.5 for high exposure and 0.3 for low exposure, and the coefficient in the flat summit is 0.2 for high, 0.1 for medium, and 0.05 for low exposure. The dry density of the manganese crusts is adopted to be 2.0.

Since the ore reserve is influenced greatly by the size of the seamount, the variation between seamounts is large. The average size of the nine surveyed seamounts is 60 $\times$ 60 km ^{2} and the dry ore reserve of their manganese crusts is 10 to 15 million tons. The total dry tonnage of the manganese crusts in the nine seamounts is 172 million tons, Co metal 1.2 million tons, Ni metal 1.0 million tons, Mn metal 39.8 million tons, Pt metal 71 tons. The metal reserve is obtained by multiplying the dry reserve tonnage by the metal content.

The overall evaluation about the characteristics of crusts occurrence and the ore reserve suggest that the seamount MS01 and MS02 are most superior among the nine seamounts and also the seamount MS03, MS04, and MS08 are relatively superior.

Table 5-8-1 Characteristics of occurrence of manganese crusts

Seamount	Scale	Topographic roughness	Gradient of flank	Water depth of summit	Exposure at flank (coeff.)	Exposure at flat summit (coeff.)	Average thickness	Co content	Pt content	Dry weight (mill. ton)	Characteristics Advantage (upper sentence) / Disadvantage (lower)
MS01	middle	little	24°	1,040m	high (0.5)	high (0.2)	3.3cm	0.67%	455ppb	15	Exposure is totally high, roughness is little, thickness is thick. Flank gradient is steep.
MS02	middle	little	19°	1,330m	high (0.5)	high (0.2)	2.4cm	0.70%	477ppb	15	Exposure is totally high, roughness is little. Flank gradient is somewhat steep.
MS03	big	moderate	10°	1,740m	low (0.3)	low (0.05)	3.0cm	0.62%	565ppb	42	Pt content is high, thickness is somewhat thick. Exposure is totally low, water depth is deep.
MS04	middle	much	15°	980m	high (0.5)	moderate (0.1)	1.8cm	0.76%	330ppb	12	Exposure at flank is high, water depth is shallow. Roughness is much.
MS05	small	much	21°	950m	high (0.5)	- (0)	1.7cm	0.91%	425ppb	2	Exposure is high, Co content is high, water depth is shallow. No flat summit. Flank gradient is steep, roughness is much.
MS06	small	little	22°	1,580m	high (0.5)	low (0.05)	1.9cm	0.76%	364ppb	6	Exposure at flank is high, roughness is little. Exposure at flat summit is low, flank gradient is steep.
MS07	small	much	16°	1,750m	high (0.5)	- (0)	1.7cm	0.83%	441ppb	6	Exposure is high, Co content is high. No flat summit. Roughness is much, water depth is deep.
MS08	big	moderate	8°	1,350m	low (0.3)	moderate (0.1)	2.1cm	0.70%	450ppb	63	Large scale. Flat summit is wide, flank gradient is gentle. Exposure at flank is low.
MS09	middle	moderate	19°	1,140m	high (0.5)	moderate (0.1)	2.2cm	0.71%	421ppb	10	Exposure at flank is high, water depth is somewhat deep. Flank gradient is steep.

Chapter 6 Discussion

For all seamounts, the survey provided detailed topography and formed the basis for sampling and other subsequent studies. Acoustic image maps prepared from MBES acoustic pressure measurements are highly effective for understanding the areal extent and the distribution of manganese crusts exposures on the seamount surface. It is considered to be a very useful technique for reconnaissance survey of manganese crusts.

As a result of the investigation, the existence of manganese crusts was confirmed in all seamounts surveyed. The mode of occurrence of the crusts is essentially similar in all seamounts. Thus it is proved that the manganese crusts occur widely from shallow summit down to 3,000 m water depth in all seamounts. It is a remarkable fact that manganese crusts occur below seafloor sediments which presently cover the seafloor.

The form, chemical composition, mineral composition, and other basic data about manganese crusts are believed to have been acquired through the results of various studies and analyses of the collected materials, moreover basic geologic and petrologic data regarding the seamounts sufficiently obtained.

Hein et al. (1992) inferred that the Marshall islands has the highest potential of manganese crusts, equivalent to the Micronesia, for the exploitation criteria such as topography, Co content, and crust thickness. In this survey compared to the existing surveys, similar data about the basic characteristics such as occurrence of manganese crusts, thickness, and ore grade were obtained. Though small amount of explorations was carried out in several seamounts in the existing surveys, various kinds of explorations, such as acoustic explorations, FDC seafloor observation and samplings, were done in all nine seamounts in this survey, and each seamount was estimated from these results. Especially in the acoustic explorations, MBES data were applied to many-sided use and SBP and SSS by narrow-beam were used to make detailed topography. It is noteworthy that such explorations as unapplied in the existing surveys were carried out in this survey and provided useful results.

On the other hand, some problems of survey methods are necessary to be recognized for the purpose that the exploration will be effectively carried out

By FDC observation, the distribution and the occurrence of manganese crusts can be clarified, but the information of their thickness is unknown, and the width of observation is at the most 3 m. The advantage of LC sampling is the availability of vertical data in spite of pointed information. Because of the function of the sampler, however, manganese crusts are not always collected, and even when they are collected many of them do not provide the thickness data. In AD sampling, large amount of materials is obtained and consequently available information is also large. However, easily-dredged material, such as protruded or pebbly crusts, are selectively collected and they do not represent the average information of the sampled site. In the acoustic survey, the MBES acoustic pressure image is very useful, but its accuracy

decreases in the slope areas.

As mentioned above, regarding survey methods, the strength and limitations of each method for the survey range and depth have been clarified. Therefore, the combination of various methods in accordance with the objective would be very important.
It is evaluated that overall analysis from various kinds of methods provided sufficient results at the stage of this reconnaissance survey.

The future subject would be in assessing the areal extent of the manganese crusts with high accuracy. In the next surveys, it is desirable, rather than investigating new seamounts, to select some from the nine seamounts surveyed by this study and to carry out the following studies.

* Prepare high-precision acoustic pressure images with topographic correction from MBES survey in order to get the accurate information on the occurrences of manganese crusts.
* Carry out SSS and FDC surveys on flat summits and FDC survey on the slopes in dense track lines, in order to complement the MBES survey results.
* Collect the samples in the bonanzas zones confirmed from the above surveys, not doing regionally on the average. The main equipment used would be AD.

Chapter 7 Summary

In 1996, the second year of the third phase of the five-year SOPAC Program, topographic surveys and sampling for manganese crust deposits were carried out in the exclusive economic zone of the Republic of the Marshall Islands. The duration of the survey cruise was 52 days.

There are some oceanic islands, atolls and many seamounts in the survey area. These largely belong either to the Ralik Seamount Chain which is aligned in the northwest-southeast direction in the western side of the area, or to the Ratak Chain aligned in the NNW-SSE direction on the eastern side.

The survey was composed mainly of bathymetric cruise of each seamount in order to clarify the detailed nature of the morphology and of sampling by large corer (LC) and arm dredge (AD) with the objective of confirming the mode of occurrence of the crust deposits. Also seafloor observation and photography by FDC were carried out for clarifying the continuity of the deposits, the type, thickness, density, grade, exposure ratio, and other relevant features of the manganese crusts. Important samples were studied in laboratories on land by various methods including; chemical analysis, X-ray diffraction, and microscopy. These together with the results of onboard analysis provided the basis for resources assessment. nSBP survey together with MBES was carried out in order to clarify the conditions of the sediments, and for some of the seamounts, SSS survey was conducted for understanding the microtopography of the seafloor.

Bathymetric survey

Nine seamounts were selected for survey after considering, the water depth, size, location, and other relevant factors. During Leg 1, four seamounts aligned in the east-west direction along the same latitude (about 14 ° N.), and located in the western part were studied. During Leg 2, five seamounts surveyed were located in the eastern part of the survey area and aligned in the southeast-northwest direction. Of the total of nine seamounts studied, seven were flat-topped, and two had pointed summits.

The areal extent of the survey differed by the size of the seamount and the results, but was about 60 x 60 km for each seamount. For all seamounts, the survey provided detailed topography and formed the basis for sampling and other subsequent studies.

The water depth of the seamount summits are 950 ~ 1,750 m, the largest seamount is MS08 extending 130 km east-west and over 100 km north-south. The relative height ranges from 3,100 m to 5,500 m.

There are no apparent relations among; the location, the movement of the Pacific Plate at the time of the formation, and topography of the seamounts. Also there are no apparent differences between the seamounts of the Ralik Chain and the Ratak Chain.

MBES acoustic reflection images

It is seen from MBES acoustic reflection images that, as a whole, in all seamounts, manganese crusts are extensively exposed along the edges of the top ridges on the slopes, and the valleys, in other words in areas where the slope is steep. Regarding individual seamounts, for example, it is seen that although MS09 has a relatively small top area, the crust exposures occupy a larger portion compared to other seamounts. Also it is seen that although MS03 has the largest flat top, most of the area is covered by foraminifera sand.

MBES acoustic reflection images are very useful, particularly for seamounts, in regional study of the areal extent and distribution of the manganese crusts efficiently.

nSBP survey

Of the flat summit seamounts, acoustically transparent layers are most developed in MS03 and they are distributed extensively to the summit edges. It is inferred from the FDC seafloor observation that zones of transparent layers are unconsolidated sediments, and all the flat summits of the seamounts are covered by sediments (foraminifera sand), with thickness ranging from 5 m to 70 m, and attaining 200 m maximum in MS03. There are parts with very thin sediments such as in the steps in MS01 and MS02 (particularly in MS02), but the flat summits of MS03 and MS04 are inferred to be wholly covered by sediments.

Most of the slopes of the seamounts are exposed, but some terraces of the slopes are probably covered by 10 ~ 20 m of sediments.

On the other hand, pointed seamounts, MS05 and MS07, are almost all acoustically opaque and there are no records indicating sediment cover.

SSS survey

It has been shown that SSS images (reflection intensity distribution) generally agree well with the MBES acoustic reflection images, and FDC observation and other methods have shown that the high acoustic pressure zones are correlated to rock (crust) exposures. The present survey results were similar. Also this method enabled very detailed and precise determination of the acoustic pressure distribution, such as the confirmation of locally low reflection acoustic pressure zones within high acoustic pressure area and the determination of thin sediment cover on the slopes. This method thus played important roles in determining the sampling sites and other precise work.

FDC survey

FDC was used for seafloor observation, and one to two track lines were set for parts of each seamount where the acoustic pressure images were high and thus the possibility of crust exposures was good. These were mostly at the summit margins and slopes (ridges, valleys). FDC was towed at ship speed of about 1 knot and important parts were photographed in color. The direction of the tow was determined by considering the wind and current directions.

Detailed conditions of the sediments and the seafloor, and distribution and continuity of the crusts were confirmed by this method. It was confirmed that the crusts were developed particularly from the summit margins to the slopes, and the relation of the topography and sediments and crust distribution and the crust types were clarified.

Sampling

An average of 15 samples were collected from each seamount by arm dredge and large corer. The targets of the sampling were manganese crusts and bottom materials. In all the seamounts surveyed, manganese crusts and associated rocks were sampled by dredge, and surface manganese crusts and foraminifera sand by corer.

Mode of occurrence of manganese crusts

Existence of manganese crusts were confirmed in all seamounts surveyed by sampling and FDC observation. Thus it was clarified that manganese crusts occur on the seamounts throughout the survey area, and their modes of occurrence are now understood. The crusts are particularly developed from the summit margins to the slopes. There appears to be no clear relations between the thickness of the crusts, water depths, and locations. Also the nature of the crusts does not vary by seamounts. The average thickness of the crusts of the collected samples is 21 mm with a maximum of 105 mm.

Chemical analysis

The average grade of the samples collected from all nine seamounts by onboard chemical analysis is Co 0.73, Ni 0.58, Cu 0.11, Mn 23.08, Fe 13.89%. These values are similar to the results of the past investigations in the waters of Marshall Islands. Regarding minor elements analyzed in laboratory on land, detailed data such as the correlation among various elements were obtained. The maximum Pt grade is 1.4 ppm and average 0.4 ppm. There are some variations in the chemistry of the collected samples by the sampling sites and seamounts, but the largest factor for the chemical difference is the horizons of the crusts (inner and outer layers), and systematic chemical differences are not caused by location of summits, topography or the nature of substrates.

Assessment

Each seamount was given a relative rank based on; its size, morphology, degree of manganese crust exposure, average thickness of the crusts, and the grade of ores. Then the ore reserves were calculated. The seamounts were assessed on the basis of these data.

The ore reserves of the average seamount surveyed (60 x 60 km) are 10 to 15 million tons. The Co, Ni, Mn, Pt metal contents of the ores are 1.2 million tons, 1 million tons, 39.8 million tons, and 71 tons respectively. A comprehensive analysis indicate that MS01 and MS02 are most promising in the area.

Summary of discussion

As a result of the present investigation, existence of manganese crusts was confirmed in all seamounts surveyed. The mode of occurrence of these crusts is essentially similar in all seamounts, and it is inferred that the crusts occur in all seamounts with summits shallower than 2,000m in the survey area.

Regarding survey methods, the strength and limitations of various methods have been clarified. Therefore, the combination of various methods in accordance with the objective would be very important, and the methods used during the present survey attained their objectives sufficiently at the present stage.

It is deemed desirable to select some seamounts from the nine surveyed and to survey them with higher accuracy rather than targeting on new seamounts. The important theme of the future survey would be the accurate clarification of the areal extent of the crusts. Preparation of high precision acoustic pressure images, SSS, FDC surveys with densely-spaced track lines would be effective.

[REFERENCES]

Brevart O., B. Dupre and C.J. Allegre, 1981, Metallogenesis at spreading centers; lead isotope systematics for sulfides, manganese-rich crusts, basalts and sediments from Cyamax and Alvin areas (East Pacific Rise). Econ. Geol. Bull. Soc. Econ. Geologists., 76, 5, p. 1205-1210.

De Carlo E.R. and C.M. Fraley, 1992, Chemistry and mineralogy of ferromanganese deposits from the equatorial Pacific Ocean., Geology and offshore mineral resources of the central Pacific basin, p. 225-245.

Hart S., 1984, A large scale anomaly in the Southern Hemisphere mantle. Nature 309, 753-757.

Haynes B.W. and M.J. Magyar, 1987, Analysis and metallurgy of manganese nodules and crusts., Marine Minerals, p. 235-246.

Hein J.R., M.S. Schulz, and L.M. Gein, 1992, Central Pacific cobalt-rich ferromanganese crusts: Historical perspective and regional variability., Geology and offshore mineral resources of the central Pacific basin, p. 261-283.

Hein J.R., W.C. Schwab and A.S. Davis, 1988, Cobalt-and Platinum-rich ferromanganese crusts and associated substrate rocks from the Marshall islands., Marine Geology, v.78, p. 255-283.

Hein J.R. et al., 190, Geological, Geochemical, Geophysical, and Oceanographic Data and Interpretations of Seamounts and Co-rich Ferromanganese Crusts from the Marshall Islands, KORDIUSGS R.V. Farnella Cruise F10-89-CP.

Janney P.E. and P.R. Castillo, 1996, Basalts from the central Pacific basin: Evidence for the origin of Cretaceous igneous complexes in the Jurassic western Pacific., vol.101, no. B2, p. 2875-2893.

Lincoln J., M.S. Prigle and I.P. Silva, 1993, Early and late Cretaceous volcanism and reef-building in the Marshall Island. in The Mesozoic Pacific; Geology, Tectonics, and Volcanism., Geophysical Monograph 77.

Mangini A., P. Halbach, D. Puteanus, and M. Segl, 1987, Chemistry and growth history of central Pacific Mn-crusts and their economic importance., Marine Minerals, p. 205-220.

Sharma P. and B.L.K. Somauajulu, 1982, 10Be dating of large manganese nodules from world oceans., Earth ahronology, Earth Planet. sci. Let., v.36, p. 359-362.

Usui A., 1995, Studies of marine manganese deposits: Review and perspectives., Chishitsu News, no. 493, p. 30-41. (Japanese)

Verma S.P., 1992, Seawater alteration effects on REE, K, Rb, Cs, Sr, U, Th, Pb and Sr-Nd-Pb isotope systematics of Mid-ocean ridge basalt. Geochem. Jour., 36, 159-178.

Woodhead J.O. and C.W. Devey, 1993, Geochemistry of the Pitcairn seamounts, I: source character and temporal trends. Earth Planet. Sci. Left., 116, 81-99.

Zindler A. and S. Hart, 1986, Chemical geodynamics. Ann. REv. Earth Planet. Sci., 14, 493-571.